



Cite this: *J. Mater. Chem. B*, 2025, 13, 4252

Urease-coupled systems and materials: design strategies, scope and applications

Shashikumar Haranal,[†] Vinay Ambekar Ranganath[†] and Indrajit Maity *

Synthetic systems have co-opted urease, a crucial enzyme serving many biological functions, to recapitulate complex biological features. Therefore, the urease-urea feedback reaction network (FCRN) is reciprocated with soft materials to induce various animate-like features, including self-regulation, error correction, and decision-making capabilities, that are processed through a variety of non-linear functions. Although free-urease-based homogeneous systems are capable of adhering to many non-linear characteristics, they lack the ability to showcase the diffusion-controlled spatiotemporal phenomena. Therefore, it demands urease immobilization, whereby a compartmentalized reaction hub can facilitate the interplay of FCRN with reaction diffusion to regulate the system's operation, allowing various non-linear responses and spatiotemporal self-organization. Indeed, the beneficial framework of urease-based commercial systems in modern technology necessitates the accessibility, reusability, and long-term stability of urease. Consequently, several techniques for urease immobilization merit attention. This review highlights the diverse covalent and non-covalent approaches for urease immobilization on different substrates and illustrates several chemical reactions and non-covalent interactions as tools for creating targeted systems and soft materials to realize many on-demand functions. We also emphasize how the advancement of systems chemistry has propelled research in soft materials to comprehend system-level applications by demonstrating several emerging non-linear functions with potent applications in many directions, including sensing, soft robotics, regulation of material properties and many more.

Received 26th December 2024,
Accepted 22nd February 2025

DOI: 10.1039/d4tb02853h

rsc.li/materials-b

Centre for Nano and Material Sciences, Jain (Deemed-to-be University), Jain Global Campus, Bangalore-562112, Karnataka, India.

E-mail: maityindrajitchem@gmail.com, indrajit.maity@jainuniversity.ac.in

[†] Equal contribution.

1. Introduction

Enzymes are the essential bio-macromolecules that serve a variety of functions, including metabolic, transcription–translation, and



Shashikumar Haranal

Shashikumar Haranal is a PhD Scholar in the RNSM Research Group at the Centre for Nano and Material Sciences (CNMS), Jain University, Bangalore, under the supervision of Dr Indrajit Maity. He earned his master's degree in chemistry from Rani Channamma University, Belagavi, India, in 2023–2024. During his master's program, he conducted a significant research project on the biogenic synthesis of copper quantum dots for sewage water treatment and dye degradation. Currently, his PhD research is centered on supramolecular polymers, self-assembly, and hydrogels.



Vinay Ambekar Ranganath

Vinay Ambekar Ranganath received his master's degree in chemistry from Adichunchanagiri University (Mandya, India) in 2022, where he did his master's project on the functionalization of halloysite for drug carriers and drug delivery. Currently, he is working as a PhD student in the RNSM research group under the supervision of Dr Indrajit Maity at the Centre for Nano and Materials Science (CNMS) at Jain University (Bengaluru). His research focuses on enzymatic pH-feedback systems and soft functional materials.

many other processes, to maintain homeostatic states.^{1,2} In the current days, with the advancement of biotechnology, enzymes display a crucial role in discovering new therapeutics against a wide range of diseases, including genetic diseases, cancer, infectious diseases, and many others.³ Additionally, outside biotechnological applications, these are utilized in other sectors, including environmental remediation, food technology, and other commercial industries, owing to their high efficiency, specificity, selectivity, and ease of handling in accordance with green chemistry principles.⁴ Numerous enzymes, such as amylase, pepsin, lipase, esterase, phosphatase, urease, glucose oxidase, laccase, and alcohol dehydrogenase, are capable of achieving these aims in contemporary industrial applications.^{5–7} Because of its tunable kinetics, simple handling, and desire-specific applications in the real synthetic world, urease is one of the most studied enzymes among them.⁸

Urease, which is basically a nickel metalloenzyme, is essential for many bacterial, fungal, and plant metabolisms and nitrogen fixation because it can catalyze the breakdown of urea into ammonia and CO₂.^{9,10} As an example, urease catalyzes the degradation of urea in *Helicobacter pylori* bacteria through their metabolic pathway, raising the pH locally to protect them from the surrounding harsh acidic environment.¹¹ In fact, the bloodstream, urine, alcohol, natural water, and other substances all contain urea, which is a toxic substance.¹² Degradation of urea is indeed the most effective method of removal. However, urea is a very thermodynamically stable molecule that needs a high temperature for decomposition.¹³ This method inevitably holds limitations for biological systems. In this circumstance, urease offers a practical and effective alternative technique for room-temperature urea elimination. Additionally, urease is a crucial diagnostic biomarker for the early detection of a number of diseases, such as gastrointestinal and urinary disorders, pyelonephritis, malignancy, and others.^{14,15}

Significantly, urease plays a key role in modern chemistry research, particularly in systems chemistry.^{16–18} It allows for the non-linear manipulation of a system's pH through a urease-urea feedback-controlled reaction network (FCRN), which can be used to control a variety of chemical and physical processes, such as catalysis, optical properties, and the self-assembly of small molecules and nanomaterials.¹⁹ To be more precise, the urease-urea pH feedback system is one of the candidates for developing artificial chemical and material systems that imitate non-linear complex biogenic properties among other enzyme reaction networks, DNA-RNA, peptide, and small molecule-based reaction networks.^{20–28} A homogeneous urease-urea network operating within a flow reactor can induce oscillations in the system's pH.²⁹ Furthermore, integrating a urease-mediated pH feedback system with an antagonistic reaction pathway could yield an autonomous system's configuration where it can successively switch the system's pH between high pH and low pH states.^{30–33} In the next step, homogeneous pH-autonomous systems possess significant potential to interact with other soft (nano)material systems, enabling the modulation of their properties for the development of life-like materials with programmable lifespans. On the other hand, FCRNs and reaction diffusion-based spatiotemporal events are critical to addressing many biological phenomena like cell-to-cell communication, biological patterns, and even biogenic motions.^{22,34} Although free-urease-based homogeneous systems can demonstrate numerous intriguing non-linear functions, they are constrained in their capacity to display reaction diffusion phenomena like chemical communication, pattern formation, and other forms of chemical morphogenesis. The compartmentalized reaction may provide the ideal configuration for integrating the processes of reaction diffusion with a feedback mechanism, facilitating the development of lifelike material systems with enhanced functionality. Along with the aforementioned constraints of free-urease-based systems for designing materials, several difficulties in terms of poor stability, storage issues, and the non-reusability of free-urease have been encountered by modern technology-based industries on a daily basis. All these constraints set a boundary for the widespread applications of homogeneous urease-based systems.^{35,36} In order to improve the enzymes' effectiveness, lifetime, and cost-effective formulation, the immobilization of urease on a perfect solid scaffold is one alternative, which could allow for easy access to the enzymes and expand the range of on-demand functions.^{37–39}

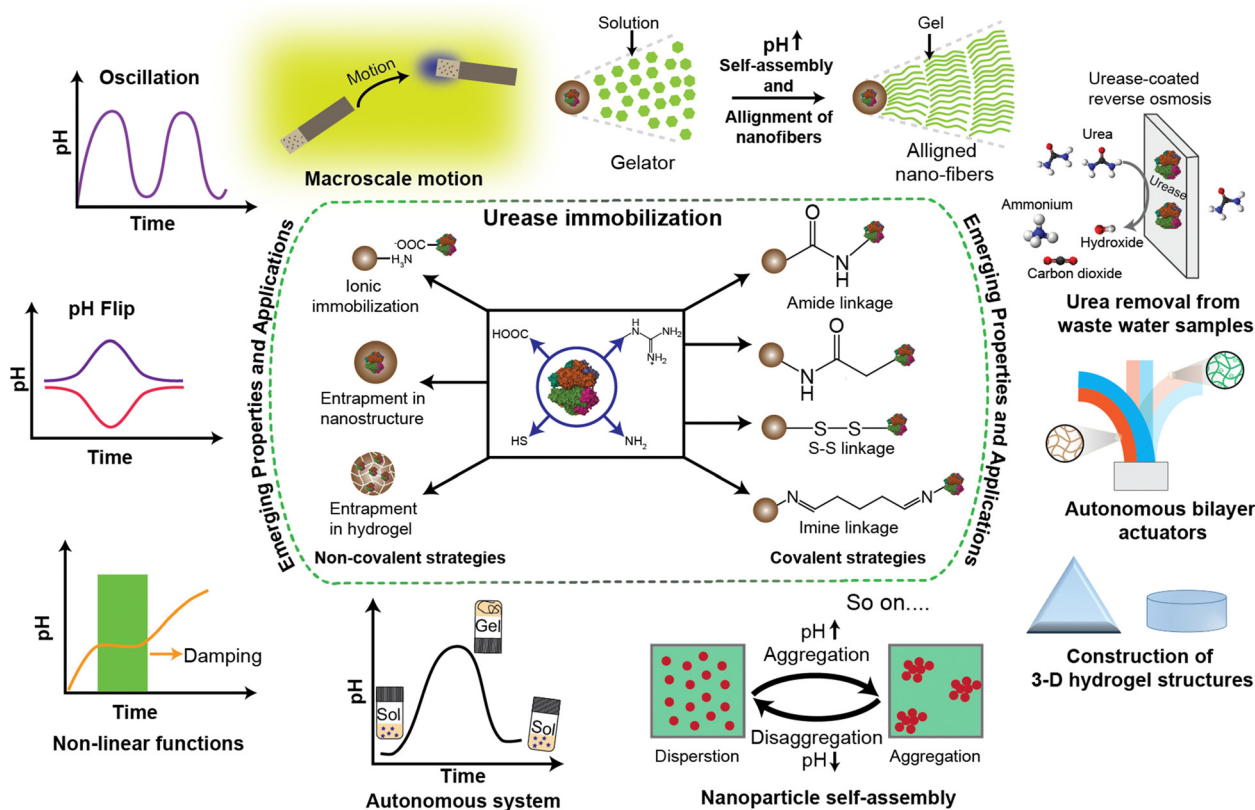
To that end, in the past few decades, various polymeric scaffolds, including chitosan, alginate, sepharose, pectin, carrageenan, collagen, cellulose, and their synthetic derivatives, solid polymeric particles, metal organic frameworks (MOFs), fibers, hydrogels, monoliths, polymersomes, or polymeric capsules, were employed to immobilize urease to achieve preferred immobilization, protection, and stabilization.^{38,40–42} Nonetheless, all these systems consist of various chemical (covalent bonding, cross-linking) and physical (adsorption, entrapment, and ionic interactions) chemistry-based methods.^{43–45} Moreover, it is highly recommended to have precise knowledge of



Indrajit Maity

Indrajit Maity is an assistant professor at the Centre for Nano and Material Sciences (CNMS) at Jain University in India. He did his PhD in organic chemistry at IIT Indore in 2015, followed by postdoctoral studies at BGU, Israel, the University of Freiburg, Germany, and JGU, Mainz, Germany. He is the recipient of many fellowships, including the PBC Postdoctoral Fellowship, the Marie S. Curie FRIAS COFUND Fellowship, the Rama-

nujan Fellowship, etc. Currently, his research group (RNSM Lab) at CNMS is focused on the field of systems chemistry, including feedback reaction networks, self-propulsion, supramolecular nanomachines, and soft materials sciences.



Scheme 1 Various immobilization strategies of urease onto the solid supports and various properties that could be included into the systems and materials to realize a variety of functions.

various immobilization techniques of urease in order to extend the prospective applications of urease-based non-linear chemical systems toward next-generation material design, which can widen and align with the scope of current technology.

Therefore, we present a concise overview of various urease immobilization strategies below. In the first section, we highlight the covalent immobilization using several chemical reactions and the prerequisites for building tailored systems for different types of sensing applications. The current history of pH feedback systems with a variety of non-trivial functionalities will then be thoroughly discussed in this review. These systems are mostly achieved by immobilizing urease non-covalently to the solid scaffolds of hydrogels or soft (nano)materials. Finally, we conclude with a critical overview, addressing the future development, prospective applications, and reach of immobilized urease-based systems. More specifically, Scheme 1 illustrates multiple methods for urease immobilization on different substrates through a variety of chemical processes and non-covalent interactions. Schematics of the different non-linear events that could result from such immobilized urease systems are presented to showcase the various emergent functionalities. These functions include pH-flip, front generation, damping, and oscillation. Interestingly, such immobilized urease systems can be easily combined with other molecular and soft (nano)-material systems to enable a wide range of applications,

including biological sensing, controlling the properties of nanomaterials, causing self-assembly towards gelation and forcing the alignment of nanofibers, creating motion toward soft robotics, and developing numerous autonomous soft (nano)material systems. After schematically providing a brief overview, we systematically demonstrate how systems chemistry (taking an example of immobilized urease systems) has propelled research in soft materials by incorporating animate features like self-regulation, autonomous operation, and decision-making abilities into the contemporary material sciences.

2. Various strategies for urease immobilization

The immobilized urease's performance is significantly influenced by the type of support scaffold used. As a result, the ideal matrix should be able to withstand physical and chemical disturbances like compression, hydrophilia, microbiological contamination, and more. Crucially, the scaffolds' pH needs to be within the ideal range. Otherwise, urease becomes denatured and loses its reactivity due to a highly acidic or basic pH. The immobilization of urease was accomplished primarily by non-covalent or covalent binding to the scaffolds, either by programming different physical forces like ionic interaction,

hydrogen bonding, van der Waals interaction, hydrophobic interaction, and π - π stacking interaction, or by employing different chemical reactions.^{46–48} In this section, we will outline the key methodologies for urease immobilization that use simple chemical processes and non-covalent interactions.

A. Covalently immobilized urease-coupled materials through various chemical reactions

a. Amide linkage. A sophisticated and simple method of immobilizing urease with its partner support scaffolds is amide linkage, which can be achieved by ligating the carboxylic acid and amine functionality. Urease consists of several amine and carboxylic acid functional groups that are non-responsive to catalytic functions but are solvent-exposed. In fact, the strategies are mostly processed by the first surface functionalization of the respective support (*i.e.*, the installation of the carboxylic acid or amine groups), followed by coupling with urease. To promote the amide coupling, one of the essential steps is to activate the carboxylic acid group using coupling reagents or active esters. Therefore, a variety of coupling reagents have been used, including DCC (*N,N'*-dicyclohexylcarbodiimide), DIPC (*N,N'*-diisopropylcarbodiimide), HBTU (1-[bis(dimethylamino)methylene]-1*H*-benzotriazolium 3-oxide hexafluorophosphate), and active esters like HOBT (1-hydroxybenzotriazole), NHS (*N*-hydroxysuccinimide), PFP (pentafluorophenol), and many more.^{49–55}

Towards this end, functionalized nanoparticles—in particular, magnetic nanoparticles (MNPs)—have been employed as an effective solid support for the immobilization of urease because they can offer easy access for purification. For instance, one of the most commonly used scaffolds for immobilizing enzymes is Fe_3O_4 NPs. A convenient method for immobilizing urease on phosphonate-grafted iron oxide nanoparticles was demonstrated by Sahoo *et al.* (Fig. 1). Their strategy involved coating

Fe_3O_4 MNPs with PMIDAs (*N*-phosphonomethyl iminodiacetic acid) and then activating PMIDAs in an aqueous buffer at pH 8 using the coupling reagent EDC (1-[3-(dimethylamino) propyl]-3-ethylcarbodiimide). Urease was subsequently added to EDC-activated carboxylic ester-appended nanoparticles to facilitate urease immobilization *via* an amide bond linker.⁵⁶ In contrast to carboxylic acid-modified Fe_3O_4 MNPs, urease immobilization could also be effectively achieved with an amine-modified support. In this case, MNPs were modified by an amino group after being covered in a silica film. Finally, by mixing the Fe_3O_4 NPs with a buffer solution that contained the coupling agent (DCC) and urease, urease was bound to the surface of amino-functional magnetic nanoparticles *via* a covalent amide bond. Most significantly, it was found that the immobilized urease's catalytic activity was preserved while its stability improved.⁵⁷

Interestingly, an EDC-based reaction was also applied for urease immobilization on the surface of polymer hydrogels, achieving long-term stability and enhancement of enzymatic activity.⁵⁸ First, a poly(acrylamide-*co*-bisacrylamide) hydrogel was prepared by the photo-polymerization technique, followed by hydrolysis of the polymer hydrogel to create active functional groups. Then urease was covalently immobilized on the surface of the polymer hydrogel *via* EDC-assisted carboxylic acid-amine coupling. Moreover, EDC/NHS was used as an efficient coupling pair for amide bond formation.⁵⁹ Fig. 2 illustrates the EDC/NHS-mediated urease immobilization on various substrates through the carboxylic acid-amine coupling reaction. Later, a polypyrrole (PPy)-based 3D porous enzyme support with good catalytic activity, stability, and reusability was also produced using the same coupling pair (EDC/NHS).⁶⁰ The carboxylic acid of PPy-COOH-coated NPs was first converted into an NHS-active ester in the presence of EDC and NHS,

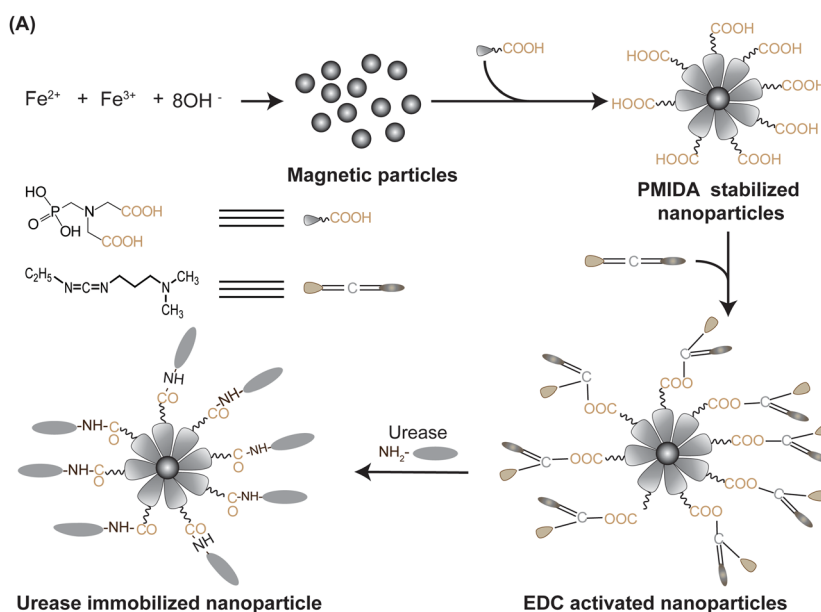


Fig. 1 A systematic approach for the immobilization of urease on PMIDAs-functionalized iron oxide nanoparticles through an EDC-mediated acid-amine coupling reaction. Adopted and reproduced under the terms of the CC-BY license, ref. 56, Copyright 2011, published by Elsevier Inc.

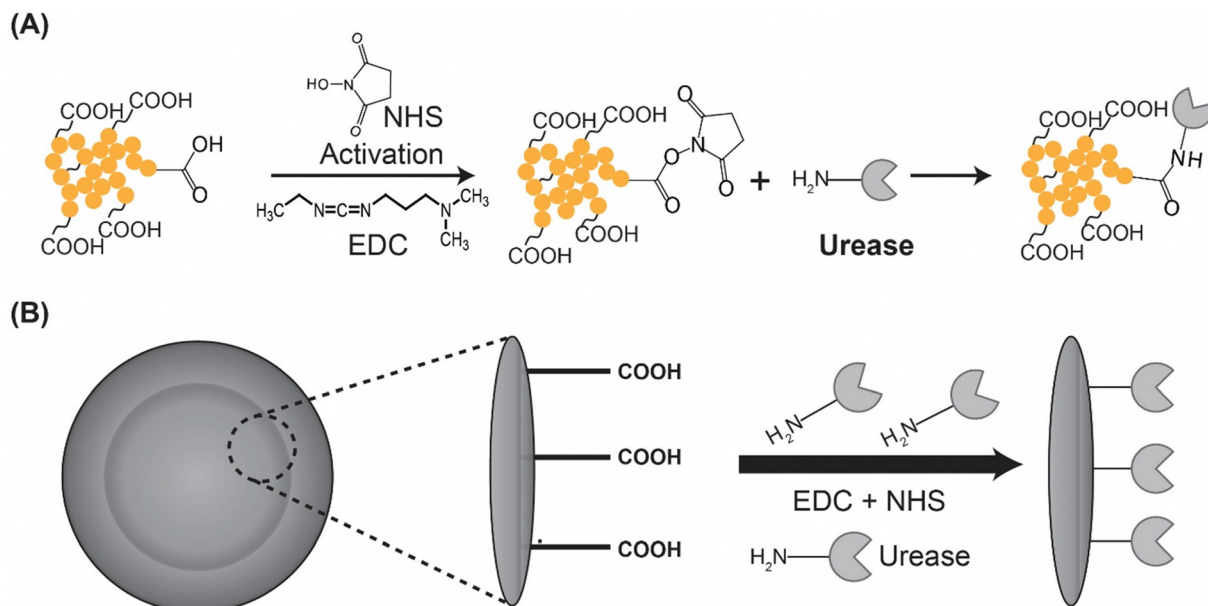


Fig. 2 (A) EDC/NHS-mediated carboxylic acid and amine coupling to construct a polypyrrole (PPy)-based 3D porous enzyme support through amide bond linkage. (B) Conjugation of urease onto the PES-PAA beads by an EDC/NHS-assisted amide coupling reaction. Adopted and reproduced under the terms of the CC-BY license, ref. 60, Copyright 2021, published by Elsevier Inc. for (A), ref. 61, Copyright 2019, published by American Chemical Society for (B).

followed by a nucleophilic substitution reaction by the amine functionality of urease, resulting in urease-immobilized 3D porous enzyme supports (Fig. 2(A)). In addition to the nanoparticle-based support, the PES (polyethersulfone)-based beads offer biocompatibility and serve as a suitable scaffold for urease immobilization. A PES-based bead was prepared by a cross-linking polymerization reaction using acrylic acid (AA) and *N*-vinyl-2-pyrrolidone (VP) as the monomers and MBA (*N,N*-methylenebisacrylamide) as the cross-linker in the presence of the radical initiator AIBN [2,2'-azobis(2-methylpropionitrile)]. The urease-immobilized PES beads were next produced by allowing the carboxylic acid-rich PES beads to react with the urease amine groups in an aqueous solution while the coupling reagent (EDC) was present (Fig. 2(B)). Interestingly, these urease-coupled PES beads were reusable and efficiently removed urea from the blood sample.⁶¹ At the same time, poly(3-hexylthiophene-*co*-3-thiophene acetic acid) (1:1; P(3HT-*co*-3TAA)) was synthesized for covalent immobilization of urease by combining the carboxylic acid groups of P(3HT-*co*-3TAA) and the amine functionalities of urease *via* a carbodiimide-based coupling reaction. The modified polymer was used to fabricate urease (Urs) electrode (Urs/P(3HT-*co*-3TAA)/ITO glass) biosensors, which detected urea at a concentration of about 5 mM by potentiometric assay.⁶² Further, membrane-based urea biosensors were also constructed using similar chemistry. More towards sensing, PVC-COOH (poly(vinyl chloride) carboxylic acid)-based ion-selective membranes (ISMII) were covalently attached to urease by using the EDC/NHS coupling protocol. This urease-immobilized membrane was efficiently used to determine ammonium ions and urea in human saliva samples.⁶³

Apart from the sensing applications, urease was covalently connected to the polymer *via* an amide linkage to achieve the urease-urea feedback-controlled reaction to enable a self-regulated and temporal control of a “breathing” microgel system (Fig. 3).⁶⁴ The microgel was made from a pH-responsive polymer called poly(*N,N*-diethylaminoethyl methacrylate) (PDEAEMA), and urease was covalently linked *via* an amide bond. PDEAEMA was first protonated, which allowed the microgel to swell upon exposure to an acidic buffer containing urea. However, the swelling was subsequently countered by the urease-mediated conversion of urea to ammonia. This increased the local pH, resulting in the deprotonation of PDEAEMA and shrinkage of the hydrogel (Fig. 3(A) and (B)). As a result, hybrid microgel breathing was feasible, which is interestingly shown to be associated with a urease-regulated fluorescence on/off switch. Fig. 3(C) and (D) show the transmission electron microscopy (TEM) images of the shrinkage and swelling states of microgels at high and low pH. The microgel swelling–shrinking cycle could be repeated by manually injecting an acidic buffer-fuel solution (Fig. 3(E)). Thus, a covalently immobilized urease system functions as an effective pH modulator, potentially regulating the physical changes of a gel material in a reversible manner.

b. Disulfide bond as a linker. The disulfide bond is a crucial motif that plays a vital role in various fields, from primordial chemistry to cellular machinery, facilitating various tasks such as protein folding into organized secondary or tertiary structures, catalysis, maintenance of oxidative stress, and others. Synthetically, urease immobilization with its partner support *via* the formation of a covalent disulfide reversible bond is one of the elegant strategies (Fig. 4). In 1974, Carlsson

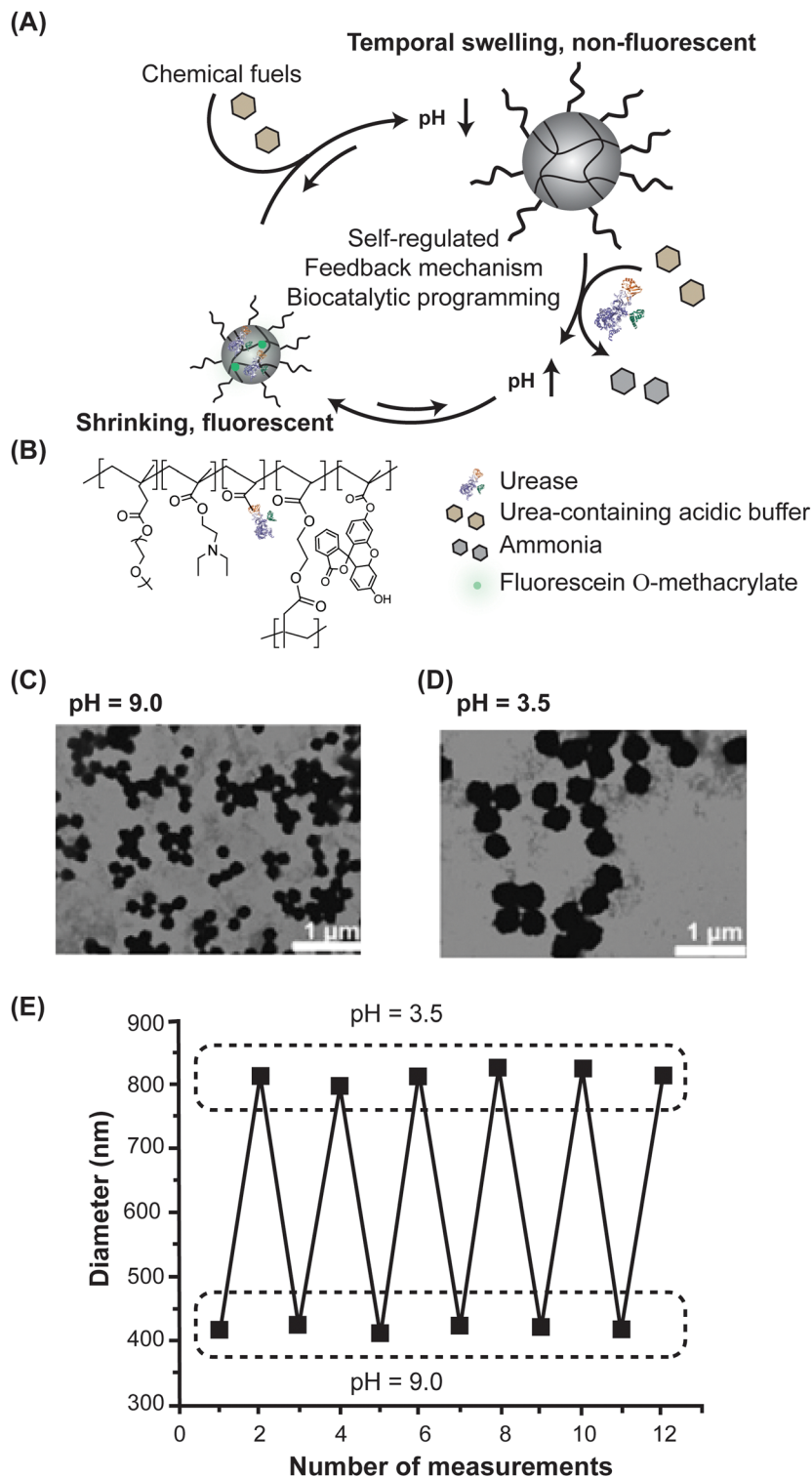


Fig. 3 (A) The self-regulated "breathing" hybrid microgel showing fluorescence on/off switch regulated by the urease-based enzymatic reaction. (B) Structure of the polymer that resulted in a hybrid microgel with covalently immobilized urease. TEM images of the hybrid microgel showing (C) shrinkage at pH 9 and (D) swelling at pH 3.5. (E) Dynamic light scattering data indicating shrinking–swelling reversibility of the microgel between pH 9 and pH 3.5. Adopted and reproduced under the terms of the CC-BY license, ref. 64, Copyright 2017, published by John-Wiley & Sons.

et al. used thiolated agarose gel beads to immobilize urease through a disulfide bond. They first prepared the mixed disulfide of glutathione-sepharose by reacting an aqueous solution

of 2,2'-dipyridyl disulfide (2-Py-S-S-2-Py) with reduced glutathione-sepharose and then slowly pumping an aqueous solution of urease through the mixed disulfide column

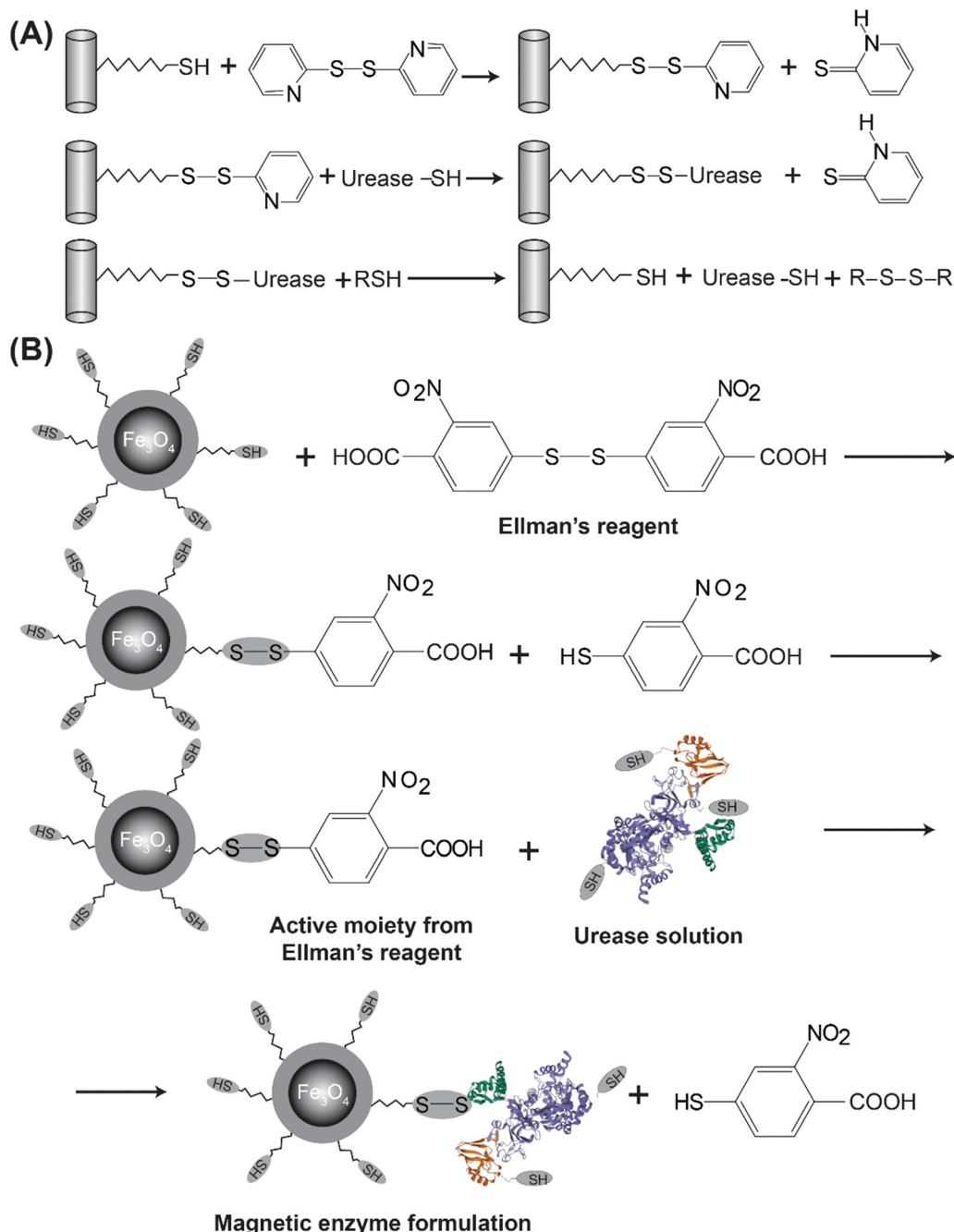


Fig. 4 (A) Urease immobilization of thiolated sepharose by reversible thiol-disulfide interchange. (B) The reaction scheme used for urease immobilization on the surface of nanoparticles with 3-mercaptopropyl groups using Ellman's reagent through the formation of a reversible covalent disulfide bond. Adopted and reproduced under the terms of the CC-BY license, ref. 65, Copyright 1974, published by John-Wiley & Sons for (A), ref. 66, Copyright 2014, published by RSC for (B).

(Sepharose-S-S-2-Py) to immobilize urease to thiolated sepharose *via* thiol-disulfide exchange (Fig. 4(A)). This simple coupling technique was followed by monitoring the synthesis of 2-thiopyridone during the reaction.⁶⁵ Furthermore, Pogorilyi *et al.* described a technique of immobilizing urease on magnetic nanoparticles coated with polysiloxane layers containing thiol- or thiol- and alkyl-functional groups.⁶⁶ The surface of siloxane-layer-coated magnetic iron oxide nanoparticles was

modified with 3-mercaptopropyl groups before being exposed to the Ellman reactant (5,5-dithio-bis(2-nitro-benzoic) acid), which produced the active moiety (Fig. 4(B)). In this stage, the urease's peripheral cysteine undergoes a disulfide exchange reaction, which results in urease immobilization on magnetic nanoparticles *via* disulfide bridges. Notably, such an immobilization method increased the residual activity of urease.

c. Immobilization via imine linkage. Likewise, the disulfide bond, another widely used methodology for reversible covalent urease immobilization, comprises the formation of a dynamic imine bond (Fig. 5). The targeted scaffolds anchored with aldehyde functionality undergo a chemical reaction with the peripheral amino functionalities of urease, resulting in covalent immobilization *via* an imine bond. In this context, nano-cellulose (NC), nanocrystals, nanofibers, and micro-cellulose (MC) were shown as the more attractive supports for urease immobilization.⁶⁷ In this regard, dialdehyde derivatives of nano- γ -Fe₂O₃@MCD (NMMCD) and nano- γ -Fe₂O₃@NCD (NMNCD) were prepared from the cotton-derived MC and NC after magnetizing them as nano- γ -Fe₂O₃@MC (NMNC) and nano- γ -Fe₂O₃@NC (NMNC) followed by periodate-mediated oxidation. In the following stage, urease immobilization on the cellulose support was accomplished by dispersing the NMMCD or NMNCD in an aqueous urease solution (phosphate buffer, 0.05 M, pH = 6) *via* an imine bond linkage (Fig. 5(A)). Another effective technique for urease immobilization on a solid support is the glutaraldehyde-mediated crosslinking process.⁶⁸ In principle, this method allows for urease immobilization on a solid support containing the amine functionality through a glutaraldehyde-amine reaction-mediated crosslinking connection.^{69,70}

Using this protocol, an enzyme-based thermistor biosensor was developed for urine analysis.⁷¹ Towards the construction of the biosensor, amine-functionalized silica gel was first activated with 2.5% glutaraldehyde in phosphate buffer (PBS, pH = 7.2), resulting in glutaraldehyde-appended silica particles, which were further treated with urease as illustrated in Fig. 5(B). The available one-terminal aldehyde group of glutaraldehyde reacted with solvent-exposed amino groups of urease to form an imine bond, which attached urease to the silica

particles. Similar chemistry was employed for the preparation of urease-immobilized porous silk fibroin (SF) membranes for biosensor purposes. The urease-immobilized membrane was achieved by following the scheme depicted in Fig. 5(C), in which the primary amine group of the SF membrane was primarily attached to a dialdehyde moiety to anchor an aldehyde group at the end by the treatment of a 10% glutaraldehyde solution with PBS at 25 °C, followed by a reaction with urease to achieve covalent enzyme immobilization *via* an imine bond.⁷² Furthermore, glutaraldehyde-assisted enzyme immobilization was also used for urease immobilization over the polystyrene ELISA plate.⁷³

Nevertheless, reversible covalent immobilization of urease allows better advantages due to the possibility of reusing the polymeric support after inactivation of the enzyme, and it may be of interest for the practical use of immobilized enzymes in large-scale processes in industry. In this context, disulfide and imine bonds serve as the conventional method for reversible covalent immobilization, providing stable linkages between the enzyme and support materials. These strategies allow for maintaining enzyme activity and stability and offer the possibility of reusability since the bonds can be cleaved to release the enzyme.⁷⁴ However, such approaches are really challenging to achieve the selective immobilization by controlling the chemical reactions. Thiol-to-disulfide reactions occur through tricky mechanisms, including ionic or radical pathways, which result in uncontrolled crosslinking of urease itself and with the solid supports.^{75,76} Similarly, the reversible immobilization through the reactive imine linkage may cause uncontrolled crosslinking. This may lead to a misorientation of the enzyme, which affects stability and activity, as the immobilization method can bury active sites. However, by applying appropriate reaction conditions, existing research has demonstrated that

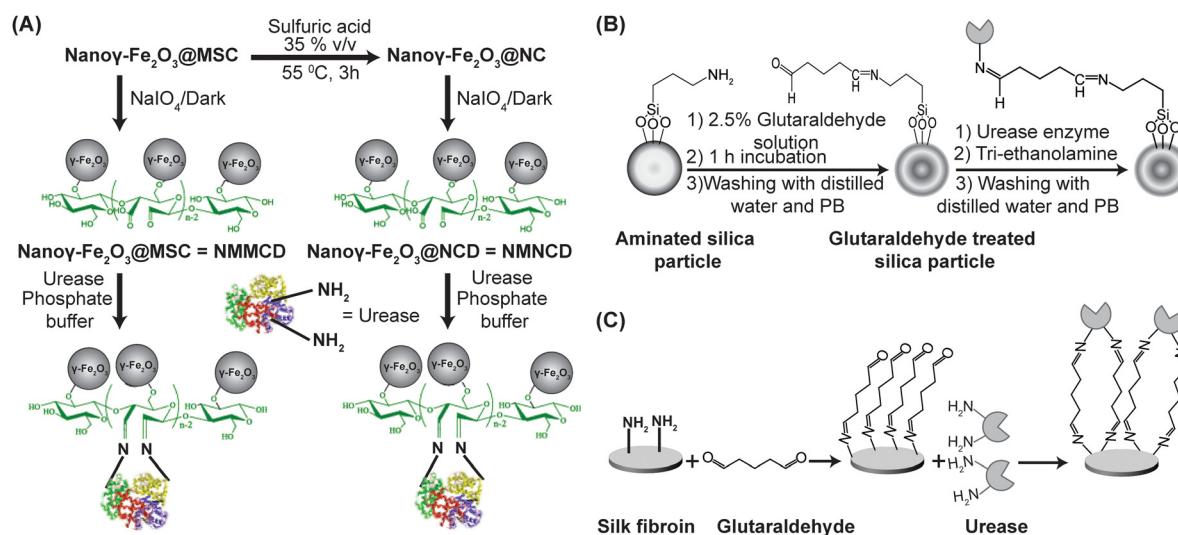


Fig. 5 (A) Covalent immobilization of urease on solid supports (NMMCD and NMNCD) *via* imine linkage. (B) Schematic representation of glutaraldehyde-facilitated covalent immobilization of urease to the aminated silica matrix. (C) A schematic representation of the immobilization of urease on the silk fibroin (SF) membrane through glutaraldehyde-mediated imine bond formation. Adopted and reproduced under the terms of the CC-BY license, ref. 67, Copyright 2020, published by Elsevier Inc. for (A), ref. 71, Copyright 2014, published by Springer for (B), ref. 72, Copyright 2018, published by MDPI for (C).

enzymes, including urease, can be immobilized *via* reversible disulfide or imine bonds and can retain their catalytic properties as well as offer the possibility of reusability.⁷⁷

d. Covalent immobilization *via* other reactions. Apart from the aforementioned strategies, several approaches are also available for covalent urease immobilization. Recently, ammonium persulfate (APS)-mediated urease immobilization was reported using different crosslinkers, divinyl benzene (DVB) and tripropylene glycol dimethacrylate (TPGDA), to generate crosslinked urease aggregates *via* a radical reaction mechanism.⁷⁸ In another methodology, a solid support anchored with an aromatic nitro moiety underwent a diazo coupling reaction with urease to covalently immobilize urease on the solid support.⁷⁹ In an alternative way, epoxy-bearing polymers are also shown to be one of the easiest and ideal systems for the immobilization of enzymes. In this regard, reactive epoxy groups bearing poly(HEMA-GMA) nanoparticles (HEMA: 2-hydroxyethyl methacrylate; GMA: glycidyl methacrylate) were used for urease immobilization *via* covalent attachment between epoxy and nucleophilic residues of the urease molecule.⁸⁰ Intriguingly, a nanomotor was recently constructed by covalently attaching urease to polydopamine nanocapsules (PDA NC) by the reaction between the amine group of urease and the catechol group of PDA *via* a Schiff base reaction for potential intravesical therapy of bladder diseases.⁸¹

Indeed, azide-alkyne cycloaddition is a very common organic reaction and a fascinating strategy for labeling and immobilization purposes. Recently, Prof. Ricci and the research group demonstrated DNA-based microswimmers driven by urease enzyme catalysis (Fig. 6).⁸² By hybridizing five distinct DNA strands with four sticky ends, they created DNA tiles that could self-assemble into hollow microtubules. Urease was then attached to the DNA microtubes' surface. Urease was initially labelled with an azide (N_3) group in order to produce the DNA-urease conjugate. The dibenzocyclooctyne (DBCO)-modified DNA oligomer was then combined with the N_3 -labeled urease in PBS buffer at pH 7.4 and left to rest overnight. Thus urease was immobilized on the DNA microtubes through the azide-alkyne cycloaddition reaction. The urease-functionalized DNA microtubes were then subjected to varying urea concentrations in order to cause motion (Fig. 6(A)). The representative trajectories of several motion experiments conducted with varying urea concentrations (0, 100, and 300 mM) are shown in Fig. 6(B) and (C). This movement is supposed to have occurred because of a gradient of ionic products (ionic self-diffusiophoresis) of ammonium (NH_4^+) and carbonate (CO_3^{2-}) around the swimmer triggered by the enzymatic reaction. Toward the deeper analysis, they extracted various motion parameters, including mean square displacement (MSD), diffusion coefficient, and speed of the motors, by using the Python-based nano-micromotor analysis tool (NMAT) v 1.0.0 44 (Fig. 6(D)). The microscale motion showed concentration-dependent behavior with the fuel urea. Fig. 6(E) and (F) display the effective diffusion coefficient and effective Δ speed, which is the difference between the speed for each condition and the speed for control conditions, as a function of urea concentration. Both effective diffusion

coefficient and speed showed a dose-dependent increase, both significantly increasing at a concentration of 300 mM. These findings unquestionably provide proof of concept for the development of synthetic DNA-based enzyme-powered swimmers that can propel themselves through fluids. Therefore, in the current day, many facile strategies are available for covalently immobilizing urease on solid supports to serve on-demand functions.

B. Non-covalent immobilization of urease onto various matrices toward the design of systems and materials

Enzymes can be combined with water-soluble polymers and dried to create immobilized enzyme products. Though this approach is straightforward, these kinds of water-soluble materials have limited applications. Therefore, different natural or synthetic polymeric materials in different physical forms—such as films, beads, coatings, gels, and different types of nanostructures—are used as support matrices in alternative methods to immobilize urease. These materials are promising because of their high mechanical adaptability and ease of fabrication. Researchers frequently study the urease-urea pH feedback system in bulk homogeneous solutions to raise the system's pH and explore its many applications; however, it fails to capture spatiotemporal events in artificial systems. Therefore, reaction networks must be connected with the physical process of reaction-diffusion control. In order to couple diffusion chemistry with FCRN and to demonstrate certain spatiotemporal self-organization structures and functionalities, a compartmentalized reaction network hub is indeed necessary. Thus, in this section, we highlight various non-covalent strategies for immobilizing urease on a variety of supports in order to develop materials with diverse functions.

a. Non-covalent immobilization through ionic interactions and extended hydrogen bonding. Nowadays, the non-covalent immobilization of an enzyme could also serve important functions. Enzymes are macromolecules containing many ionized functional groups. Many of them involve catalytic function with a proper spatial organization in the catalytic pocket, while others remain in a non-catalytic peripheral position. Therefore, knowledge of the isoelectric point seems to be vital to controlling the enzyme's functionality by programming the ionization of side chain amino acids. Charged amino acids in enzymes can engage in ionic interactions with substrates possessing opposite charges, thereby promoting non-covalent attachment to the surface. Therefore, the equilibrium between the neutral and ionized forms could be easily monitored by tuning the pH of the medium. All these properties of enzymes offer guidelines on how to design the support scaffolds, either surface-functionalized nanoparticles or polymers with perfect countercharge. The non-covalent immobilization of enzymes depends on a variety of non-covalent interactions, including hydrophobic effects, hydrogen bonds, and ionic interactions (Fig. 7). To that end, resin particles were recently functionalized by amino groups, which were employed to bind urease non-covalently and were further used to investigate the clock reaction in the urea-urease- H^+ reaction system.⁸³

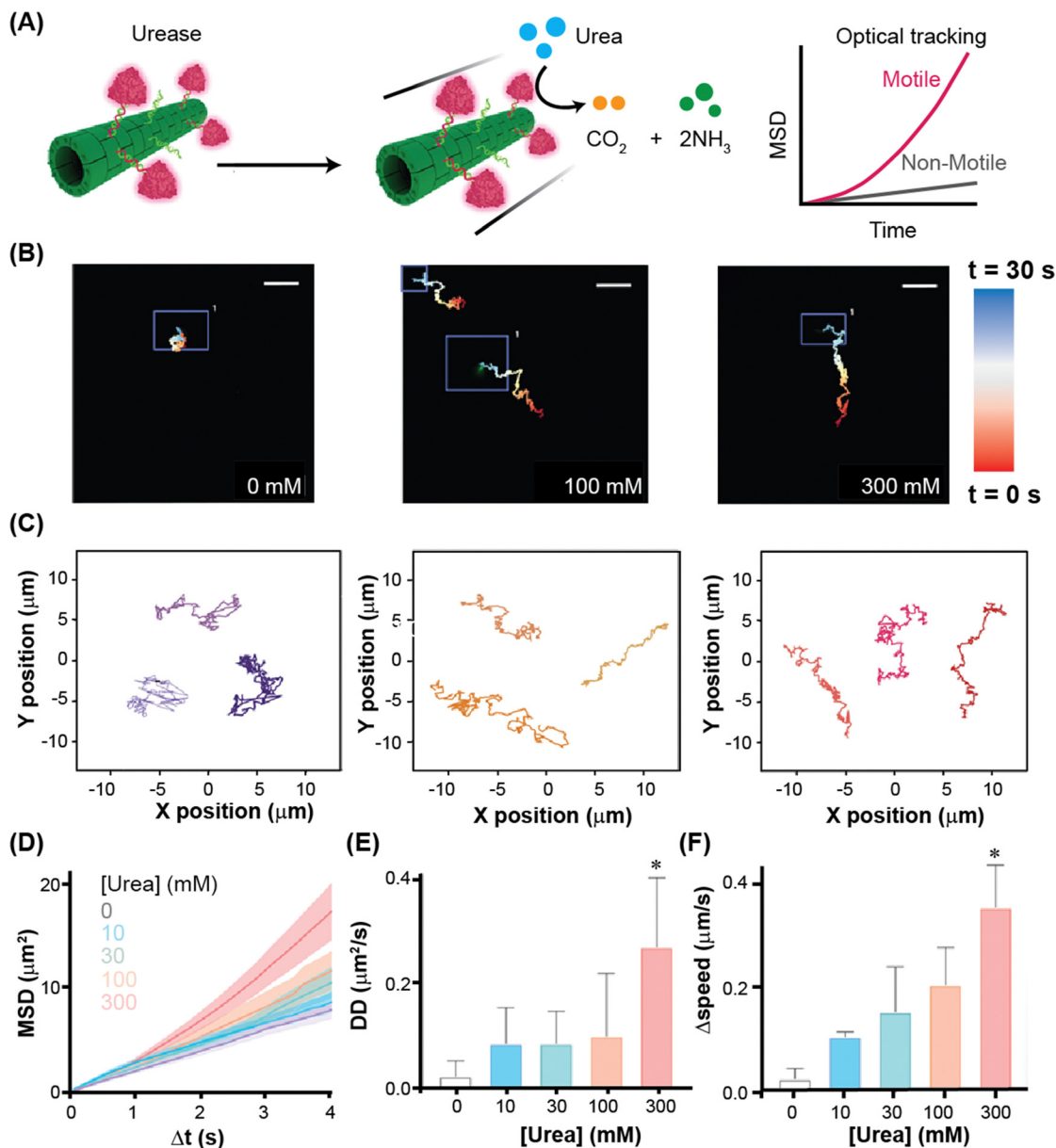


Fig. 6 (A) Schematic illustration of the mechanism of urease immobilized DNA-based swimmers. (B) and (C) Various trajectories of DNA swimmers when exposed to different urea concentrations (0, 100 and 300 mM). (D)–(F) show the variation of mean square displacement, diffusion coefficient, and speed of the motors on fuel (urea) concentration. Adopted and reproduced under the terms of the CC-BY license, ref. 82, Copyright 2024, published by the American Chemical Society.

The buffer was at pH 8, which led to a positively charged surface for the resin particles. On the other hand, the carboxylic acid groups of urease turn into carboxylate ions, providing negatively charged macromolecules. Therefore, mixing urease with resin particles in PBS at pH 8 facilitates urease immobilization on resin particles through the ionic interaction between $-\text{NH}_3^+$ and carboxylate ions (Fig. 7(A)). Moreover, by using the simple electrostatic process, a urease-immobilized ZnO nanowire electrode was fabricated for the selective determination of urea.⁸⁶ Remarkably, polymer networks bearing positive or negatively charged branches are also utilized as a good scaffold for urease immobilization. In this regard,

polymer networks obtained by mixing poly(acrylic acid) (PAA) and poly(1-vinyl imidazole) (PVI) at several stoichiometric ratios were employed for the immobilization of urease.⁸⁴ At a particular pH (pH 7.5), PAA behaves as a negatively charged polymer, whereas in PVI, the imidazole moiety converts into the imidazolium ion, and thus PVI bears a positively charged functional group. Therefore, the mixture of PAA, PVI, and urease provides a urease-polymer network matrix stabilized by strong ionic interaction among them (Fig. 7(B)). Recently, urease encapsulation in zeolite imidazolate-based framework-8 (ZIF-8) was made possible by biomimetic mineralization, which produced urease@ZIF-8 in moderate circumstances

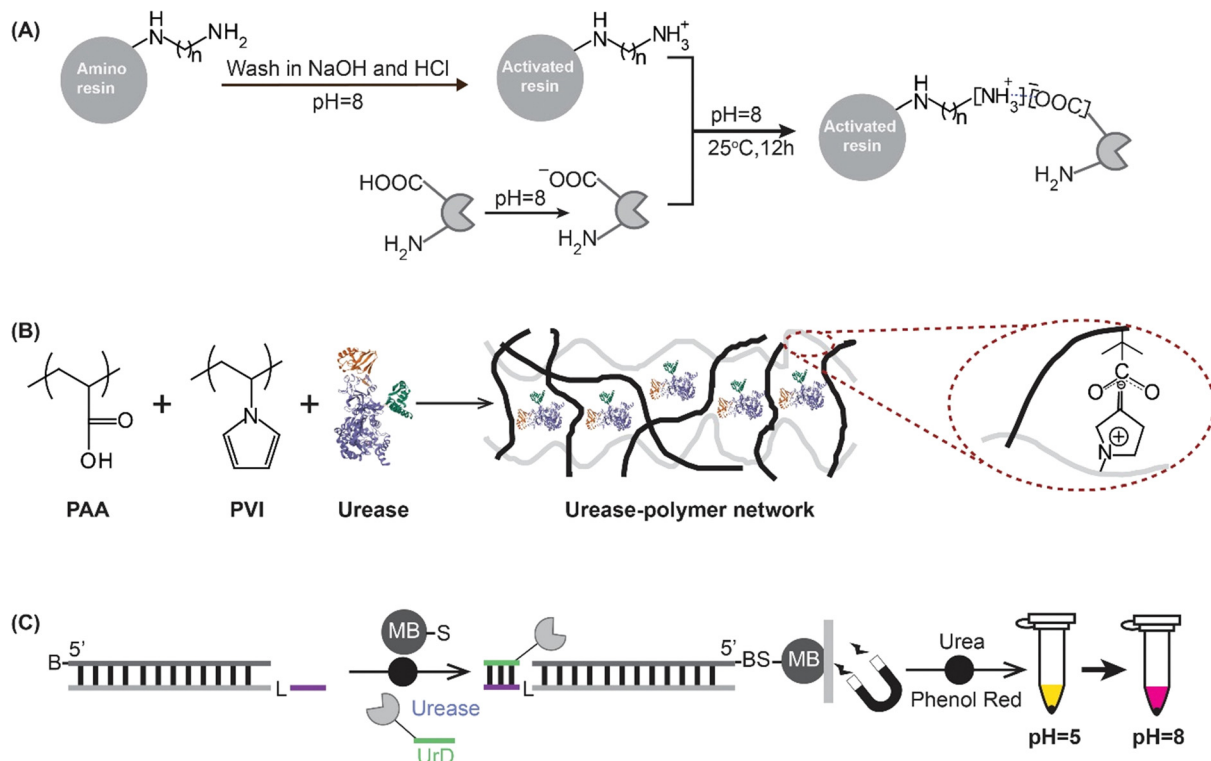


Fig. 7 (A) Urease immobilization processes by noncovalent ionic interaction between NH_3^+ and carboxylate ions. (B) Immobilization of urease into the PAA/PVI network through the ionic interaction of imidazole and carboxylate ions. (C) The immobilization strategy of urease onto magnetic beads by a DNA strand displacement reaction between a DNA gate and urease-labeled DNA driven by hydrogen bond formation. A litmus test is shown, indicating preservation of the urease activity after the immobilization. (B: biotin, L: triethylene glycol linker, S: streptavidin, MB: magnetic bead.) Adopted and reproduced under the terms of the CC-BY license, ref. 83, Copyright 2019, published by RSC for (A), ref. 84, Copyright 2010, published by Springer for (B), ref. 85, Copyright 2017, published by Springer Nature for (C).

using the same ionic interaction method.⁸⁷ However, hydrogen bonding is also known as another fascinating key to improvising the non-covalent immobilization of urease on solid supports driven by DNA hybridization.⁸⁵ In this design, two DNA sequences are connected by a triethylene glycol linker, one targeted for binding with a 5'-biotin-appended DNA primer and the second hybridized with the DNA strand (green) coupled onto urease, a conjugate denoted "UrD," as depicted in Fig. 7(c). Thereby, the resulting DNA gate-anchored urease could easily be immobilized on the surface of magnetic beads by using streptavidin-biotin conjugation. The urease-immobilized beads can then be used to change the pH of the solution from acidic to basic.

Enzyme immobilization through biotin-streptavidin linkage is also one of the attractive approaches. One of nature's most potent non-covalent interactions is that between biotin and SA (streptavidin), which is a popular method and paradigm for protein-ligand interactions and operates through strong hydrogen bonding interactions. Recently, Prof. Sen and collaborators have demonstrated how to generate the motion of macro-scale sheets powered by urease pumps.⁸⁸ Using both experiments and simulations, they showcased that the urease pumps are capable of driving centimeter-scale polymer sheets along directed linear paths and rotational trajectories on the air/water interface (Fig. 8). The moving object is a polydimethylsiloxane

(PDMS) sheet and was fabricated layer by layer in a geometry in which the outermost thin layer was coated with gold. The enzymes (urease or alkaline phosphatase) were attached to the deposited gold (30 nm thick) on a PDMS thin film (120 μm thick) through biotin-streptavidin linkages (Fig. 8(A)). Fig. 8(B) shows a simulated object's configuration to generate motion, which is made of passive beads (blue) representing the pristine PDMS film and active beads (orange) denoting the enzyme-immobilized film. An ammonium gradient and hence a local flow are produced when the enzyme-coated surface faces in the direction of the solution below, causing urease and urea to come into contact and aiding the urea hydrolysis reaction. The asymmetric coating is seen as the key to allowing the localized convective flows of the educts under the film that move the film in a specified direction. Interestingly, the film velocity was found to vary with the area of gold coverage (Fig. 8(C)). Slower movement was seen with larger or smaller enzyme coverage on the sheet, while a fully coated film generated a very slow random motion.

Only half-coated films allowed the sheet to move fast on the air/water interface. Fig. 8(D) depicts the motion trajectory of the sheet with half-coated urease. Fig. 8(E) and (F) illustrate that the sheet moves with different velocities while it is subjected to a urea solution having different amounts of urea (0, 0.02, 0.1, 0.5, and 1.0 M urea). However, it reaches a maximum velocity of

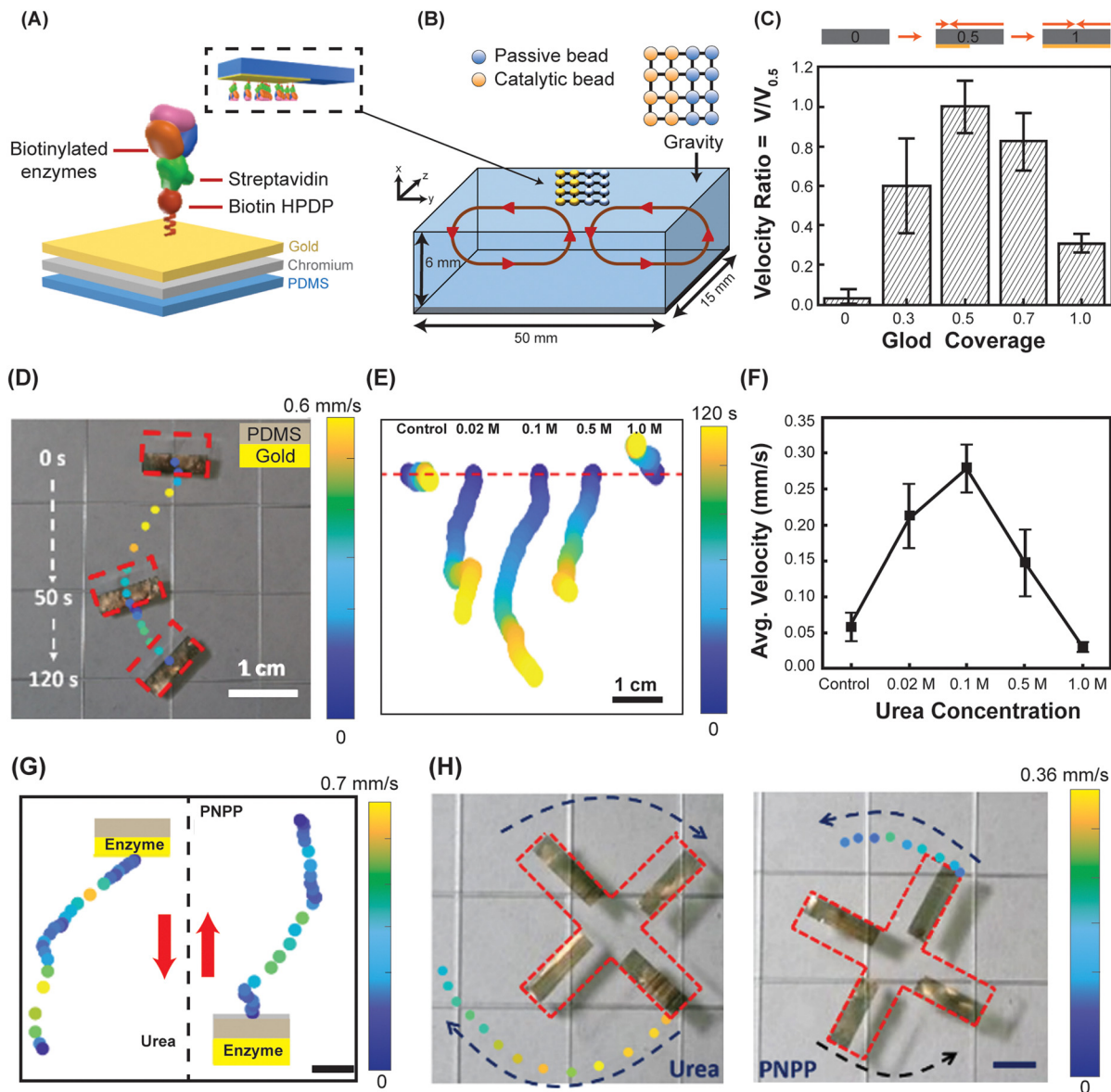


Fig. 8 (A) Urease and alkaline phosphatase immobilized layer-by-layer structured PDMS film floating on water and propelling the air–water interface. (B) Simulation setup. Passive beads (blue) indicate the pristine PDMS film, while active beads (orange) denote the enzyme-coated film. (C) Film velocity as a function of area of gold coverage. (D) Motion of a half-coated urease-immobilized film on a 0.1 M urea solution. Film positions are shown with the time intervals. (E) Urease-attached film displaying different trajectories with various urea concentrations. (F) The average velocity of the moving film as a function of urea concentration. (G) The film coated with both urease and alkaline phosphatase shows motion in different directions when tested with urea and PNPP solution, respectively. (H) The windmill-shaped film immobilized with both urease and alkaline phosphatase rotates clockwise in 0.1 mM urea and anticlockwise in 50 mM urea with PNPP. Adopted and reproduced under the terms of the CC-BY license, ref. 88, Copyright 2024, published by John-Wiley & Sons.

0.27 mm s^{-1} in 0.1 M urea solution. Subsequently, they showed that the alkaline phosphatase (AkP) immobilized sheet moves to the right in *p*-nitrophenyl phosphate (PNPP), while the urease-coated sheet moves to the left when submerged in urea, as depicted in Fig. 8(G). This suggests that both enzymes were generating fluid flows in opposite directions to one another. They further fabricated a large windmill-shaped design with arms that were partially coated with urease or phosphatase in order to facilitate the more intricate macro-scale movement. The film began to rotate clockwise when the windmill was

submerged in 0.1 M urea solution and anticlockwise when submerged in 50 mM PNPP solution (Fig. 8(H)). As a result, these findings can be used to guide the impromptu movement of soft robots and large equipment.

b. Urease immobilization in nano(micro)compartments. Nano-compartments such as micelles, liposomes, vesicles, polymersomes, coacervates, nanogels, microgels, and many more are the promising self-assembly-driven architectures at the mesoscopic length scales that are used in various fields such as drug encapsulation and controlled release, delivery

vehicles, sensing, absorbents, catalysis, and others.^{89–93} Remarkably, these compartments can entrap enzymes non-covalently and have the advantages of ease of handling, prolonged availability, robustness, enhanced resilience to environmental changes, and reusability. Taking these advantages, a lipid, 1-palmitoyl-2-oleoyl-*sn*-glycero 3-phosphatidylcholine (POPC)-based giant vesicle was prepared to encapsulate the urease enzyme and maintain the different membrane permeability (P_m) of product ammonia, fuel urea, and external proton concentrations $[H^+]$. This offers a reliable simulation approach that takes into account all physical and urease-urea feedback kinetic factors to accurately predict the prerequisites to display either sustained or damped oscillations in the temporal pH changes, which could subsequently be confirmed by experiments in an actual system.^{94,95} Recently, phospholipid 1,2-diphytanoyl-*sn*-glycero-3 phosphocholine (DPhPC)-based vesicles were prepared by the lipid film hydration and extrusion method, in which first thin films were formed by adding lipids in chloroform, followed by subjecting them to hydrating solutions containing urease, pyranine, and other substances that needed to be encapsulated for experimental requirements. In the next step, several cycles of the freeze-thawing process resulted in urease-encapsulated vesicles. Interestingly, the combined experimental and simulation approach demonstrated collective behavior, pH clocks, and fast ammonia transport with these urease-encapsulated phospholipid-based nano- and microvesicles.⁹⁶ Similarly, a polymersome based on the block copolymer mPEG₄₅-*b*-P(DEAEMA₁₃₀-*co*-BMA₁₂-*co*-FMA_{0.35}) (PEG: poly(ethylene glycol); DEAEMA: 2-(diethylamino) ethyl methacrylate; BMA: 2-hydroxy-4-(methacryloyloxy) benzophenone; FMA: fluorescein O-methacrylate) was used to accommodate both urease and horseradish peroxidase (HRP) to showcase feedback-assisted temporal control of the “breathing” phenomenon in the polymersomes.⁹⁷ To immobilize the enzymes, the block polymer in tetrahydrofuran was injected into the enzyme (urease, HRP) solution in phosphate buffer *via* a syringe pump. The resulting cloudy suspension containing polymersomes was dialyzed against water. After dialysis, the polymersome and enzyme mixture was centrifuged multiple times until the free enzymes were removed from the solution. Subsequently, the polymersomes entrapping both enzymes were collected and used in the respective experiments. With that line, the urease- and HRP-entrapped bicontinuous nanospheres were recently prepared by the same research group with a block copolymer of mPEG₄₅-*b*-p[DEAEMA₁₇₅-*g*-BMA₂₈] by using the nanoprecipitation strategy that was previously mentioned. Then, using the same protocol, they demonstrated pH control and membrane permeability by employing a urease-urea reaction that was compartmentalized in bicontinuous nanospheres (BCNs). Interestingly, such programmed membrane permeability further allowed controlled catalysis for the HRP reaction.⁹⁸

Apart from the nanoprecipitation technique, the photoinitiated reversible addition–fragmentation chain-transfer polymerization-induced self-assembly (photo-PISA) strategy was employed to obtain semipermeable polymersome nanoreactors

that could successfully encapsulate urease to produce PISA-urease. On the other hand, the self-assembly of a DASA-modified amphiphilic block copolymer (DASA: donor–acceptor Stenhouse adduct) was driven by the solvent exchange method to produce the nanoreactor that encapsulated the esterase and was capable of alternating small-molecule semipermeability states by a photoswitch. These enzyme-immobilized nanocompartments were used to demonstrate the photoswitchable gating of a non-equilibrium enzymatic feedback system and establish chemical communication among the polymersome nanoreactors.⁹⁹ Recently, various enzymes, including urease, were non-covalently immobilized in the DNA-based protocell to execute protocell logistics using an oscillatory cell-like transporter capable of repeated pick-up and delivery of molecular cargo.¹⁰⁰ Moreover, the combination of stimuli-responsive polyelectrolyte capsules and urease-immobilized microgels has been shown to mimic life-like artificial systems and their programmable interactive communications and self-regulation behavior through communication-feedback mechanisms.¹⁰¹

c. Entrapment under the synthetic gel networks. Besides the lipid- or polymer-based nanostructures, synthetic polymer hydrogels are also excellent scaffolds to entrap urease efficiently. For example, some polymer hydrogels, such as poly(ethylene glycol) (PEG), poly(2 hydroxyethylmethacrylate) (PHEMA), poly(*N*-isopropyl acrylamide) (PNIPAM), and acrylamide copolymer-based hydrogels, are widely used as scaffolds for enzyme immobilization.¹⁰² These hydrogels are preferred because of their hydrophobic/hydrophilic balance, inertness for enzymatic degradation, and high chemical and mechanical stability.¹⁰³ Taking such a non-covalently immobilized enzyme reaction hub to the next level of applications, Prof. Walther and collaborators introduced layered compartments of non-covalently immobilizing antagonistic pH-modulating enzymes in an acrylate-based polymer hydrogel and demonstrated that transient pH signals in a supernatant solution could be programmed based on spatial delays (Fig. 9).¹⁰⁴ Fig. 9(A) depicts the strategy to immobilize urease and esterase in the layer-by-layer polymer hydrogel obtained by the photopolymerization technique. The whole system comprised three layers: a urease layer (bottom), an esterase gel layer (middle) of photocross-linked poly(poly(ethylene glycol) diacrylate) (PPEGDA), and a supernatant layer (top layer) of fuels (urea and ethyl acetate (EA)) in citrate buffer. To immobilize urease and esterase in the polymer hydrogel, a mixture of poly(ethylene glycol) diacrylate (PEGDA 6000) (monomer, 30 wt%), urease/esterase (desired amount), and lithium phenyl (2,4,6-trimethylbenzoyl) phosphinate (LAP) as the photoinitiator was taken and then subjected to irradiation for 10 min by a 365 nm, 36 W UV lamp. Actually, urease and esterase immobilization was preceded by sequential layer-by-layer photoinitiated polymerization of the hydrogel, as depicted in Fig. 9(B). This sophisticated system addressed the limitations of activity mismatches of antagonistic enzymes in homogeneous solutions and was capable of programming acidic and alkaline pH lifecycles beyond the possibilities of homogeneous solutions by synchronizing the enzyme kinetics and diffusion of educts. The introduction of

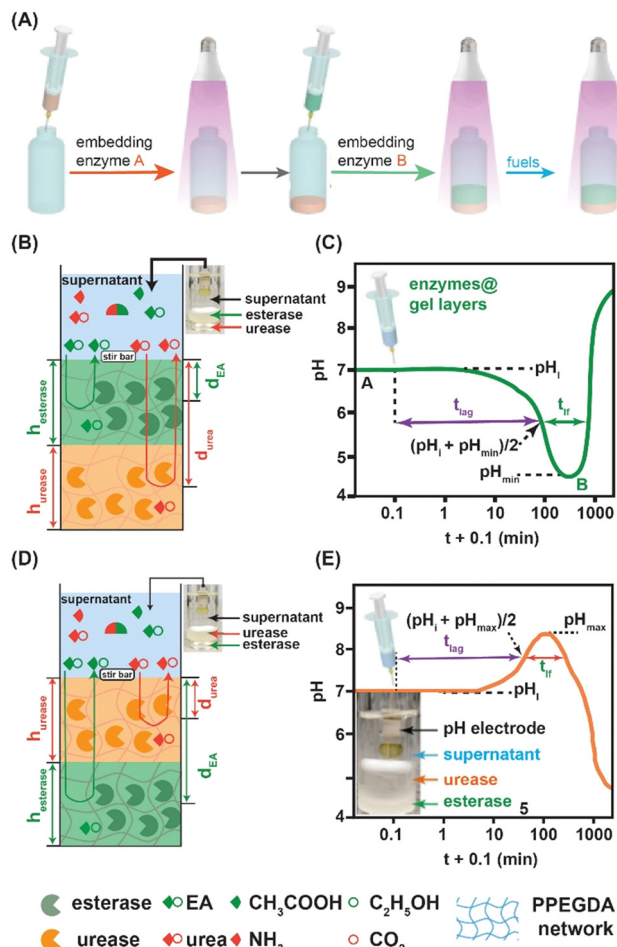


Fig. 9 (A) Urease and esterase immobilization processes in the layer-by-layer hydrogel using the photopolymerization technique. (B) The system configuration in which esterase encapsulated in the top gel layer catalyzes the hydrolysis of EA to HAC, while urease embedded in the bottom layer converts urea to NH₃ and CO₂, and the topmost solution layer contains fuel urea and EA. (C) The transient acidic pH flips resulted in configuration B. (D) The system configuration comprises urease in the top gel layer while esterase is embedded in the bottom layer, and the topmost solution layer contains fuel urea and EA. (E) The transient basic pH flips that resulted in configuration D. Adopted and reproduced under the terms of the CC-BY license, ref. 104, Copyright 2021, published by John-Wiley & Sons.

the chemical fuels in the top layer facilitated the diffusion of ethyl acetate (EA) and urea into the hydrogel layers, where they were transformed into acidic (acetic acid, HAC) and basic (NH₃) products by their respective enzyme's kinetics. Nevertheless, the temporal acidic and basic products were regulated by the differential diffusion and their kinetic disparity, which resulted in either an acidic pH flip with a system configuration having a top layer of esterase and an underneath urease layer or a basic pH flip with a top layer of urease and an underneath esterase layer (Fig. 9(C)–(E)). Moreover, this engineering approach provided ease of access to program the lag time, lifetime, and pH minima and maxima by adjusting spatial and kinetic conditions.

Further, the same group immobilized urease in the polyaspartic acid *N*-acrylamide (A3)-based hydrogel by the above-

mentioned protocol of photocrosslinking polymerization and constructed a bilayered hydrogel device coupled with an active urease-containing gel block and a urease-free passive gel block. They showcased homeostatic-like autonomous activities of soft robots guided by chemo-mechanical feedback mechanisms empowered by urease-urea chemical reaction networks.¹⁰⁵ Similarly, poly(acrylic acid-co-dimethylaminoethyl methacrylate) hydrogels were also potentially useful for the efficient immobilization of urease. In this method, a homogeneous prepolymer solution in phosphate buffer was prepared by mixing acrylic acid and dimethylaminoethyl methacrylate as the monomers, bisacrylamide as a crosslinker, and the desired amount of urease for immobilization. Next, polymerization was initiated by introducing thermal radical initiators, ammonium peroxydisulfate and *N,N,N',N'*-tetramethylethylenediamine. The pregel was completely cured by heating at 35 °C for 3 hours to ensure a strong polymer hydrogel that entrapped the urease. This urease-immobilized polymer hydrogel was employed to design a piezoresistive hydrogel biosensor for the detection of urea.¹⁰⁶

Apart from the aforementioned polymer hydrogels, the thiol-acrylate polymer hydrogel is also one of the promising matrices for the immobilization of urease toward designing materials with emerging nonlinear features. The homogeneous urease-urea batch reaction showed irreproducible oscillation due to the lack of stability. To address this issue, Prof. Taylor and the research group immobilized urease in thiol-poly(ethylene glycol) acrylate (PEGDA) hydrogel beads, which are prepared by emulsion polymerization.¹⁰⁷ This approach involved the preparation of a stock solution with a mixture of urease, ethoxylated trimethylolpropane tri(3-mercaptopropionate), polyvinyl alcohol, poly(ethylene glycol) diacrylate (PEGDA, average $M_n = 700$), and urea. When the mixture turned viscous, the solution was injected dropwise into hexane. The solution was stirred using a magnetic stirrer until hydrogel beads were formed. The urease-immobilized beads were then separated and washed for further investigations. Interestingly, these beads produced pH clock reactions similar to the batch reaction, and the non-linear pH activities were reproducible and remained unaffected over several days compared to hours with the free enzyme in water.

d. Entrapment under the biopolymer (alginate or agarose) gel networks. Outside the synthetic polymer hydrogels, many natural polymer-based beads and hydrogels, such as silk, gelatin beads, alginate, chitosan, agarose, and cellulose, are available for urease immobilization.^{37,39,41,108,109} However, to that end, in most cases, the urease was non-covalently entrapped into the gel matrix of natural polymers (alginate or agarose) by using many convenient strategies. Along that line, urease immobilization into an alginate hydrogel sphere was shown to be an efficient but simple approach to constructing many systems with interesting functions. Recently, Maity *et al.* reported feedback, communication, and engineering of hydrogel structures by using enzyme-loaded alginate gel spheres (Fig. 10).¹¹⁰ This strategy of urease immobilization into an alginate gel sphere involved preparing a well-mixed urease-alginate viscous solution in an aqueous medium, followed by

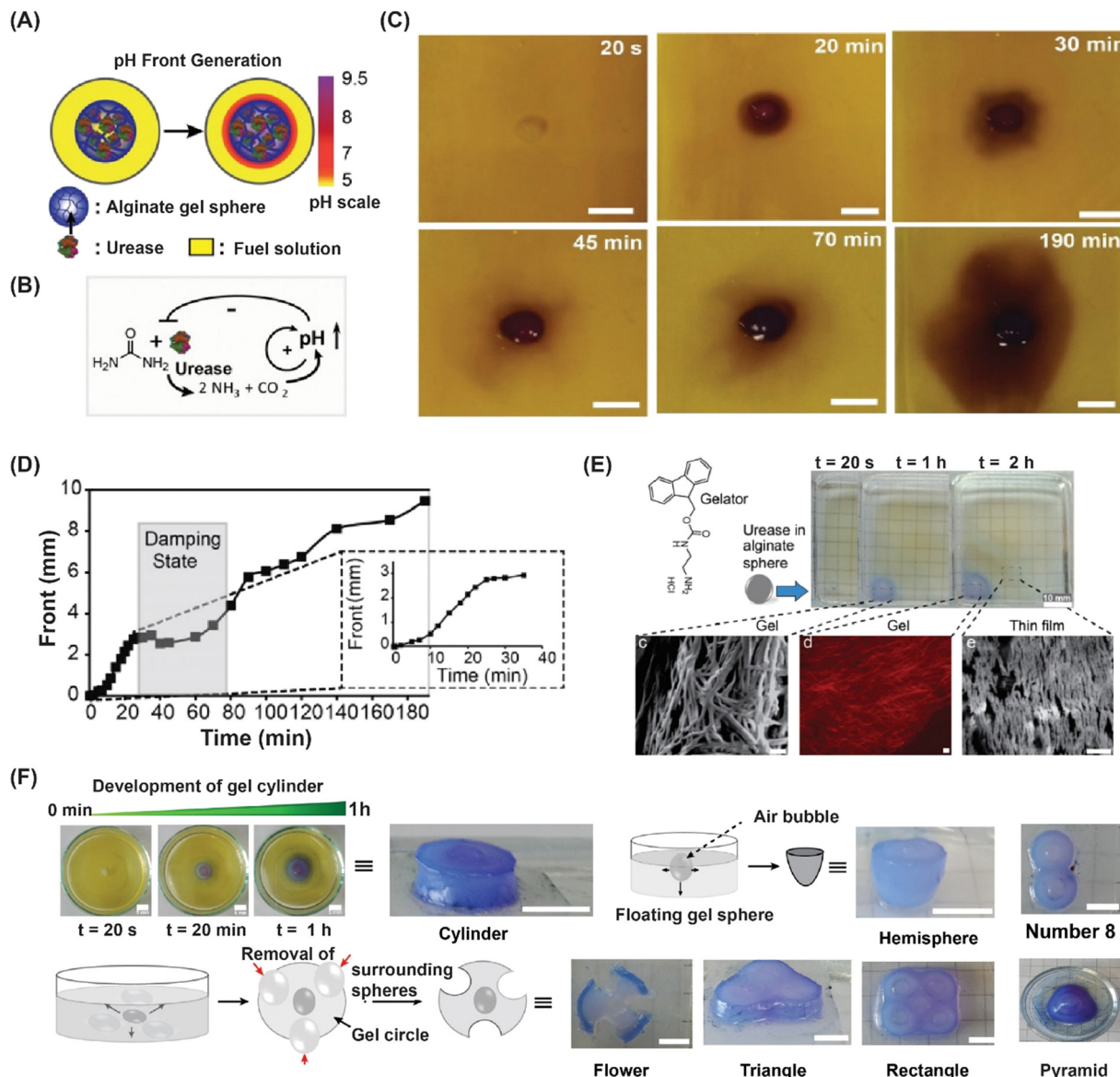


Fig. 10 (A) A pH front generated by placing a urease-loaded alginate gel sphere into a solution containing urea (300 mM) in citrate buffer (10 mM Na₃C/CA, pH 3.5). (B) Urea-urease network topology. (C) Time-lapse photographs of the basic pH front from a compartmentalized urease-urea reaction network (0.6 g L⁻¹ urease), highlighting the non-linear damping phenomenon. (D) The initial sigmoidal signature and later damping phenomena achieved by processing the propagation of the basic pH front shown in (C). (E) Growth of the self-assembled gel front of the gelator (Fmoc-EtNH₂) guided by the basic pH front generated by the urease-loaded sphere (radius = 1.05 mm, 9 g L⁻¹ urease). The respective SEM (scanning electron microscope) images show the alignment of nanofibers. (F) Autonomous growth of various geometrical hydrogel structures, including cylinder, hemisphere, number eight, flower, triangle, and rectangle. A more complex 3D pyramid was constructed by layer-by-layer deposition of the gel material by the pre-patterns of urease-loaded gel spheres. Gelator-fuel solution: 4 g L⁻¹ Fmoc-Et-NH₂, 300 mM urea, 10 mM Na₃C/CA (pH 3.5), 0.05 g L⁻¹ BCP. Scale bars: 5 mm. Adopted and reproduced under the terms of the CC-BY license, ref. 110, Copyright 2021, published by John-Wiley & Sons.

adding droplets of the urease–sodium alginate mixture into an aqueous solution of CaCl₂ (100 mM) by a syringe.

The alginate gel spheres entrapping urease were produced within 10–15 minutes by the formation of a polymer network through the Ca²⁺ ion-mediated crosslinking of alginate polymers. This compartmentalized urease reaction was investigated to generate a basic pH front while immersed in the fuel solution containing fuel urea and pH-readable dye, bromocresol purple (BCP), in Na₃citrate/citric acid buffer (Na₃C/CA;

pH 3.5) (Fig. 10(A) and (B)). The urease-urea feedback-controlled reaction network tethered with positive and negative feedback enables the uncovering of the non-linear responses of the system by coupling with diffusion chemistry, as illustrated in Fig. 10(B)–(D). This system configuration delivered the advantages of controlling the self-assembly of a small-molecule gelator (Fmoc-ethylenediamine hydrochloride, Fmoc-Et-NH₂) to yield a hydrogel with the formation of aligned nanofibers (Fig. 10(E)). More importantly, the interplay of the pH front and

diffusion chemistry leveraged a facile approach for self-synthesizing various types of 2D and 3D hydrogel structures as an alternative to 3D printing tools (Fig. 10(F)).

Similar system configurations of urease-loaded millimeter-sized alginate beads were constructed by Jagers *et al.*, in which they demonstrated short-range chemical communication in an aqueous environment in the presence of silver cations (Ag^+) and their chelator dithiothreitol (DTT) as signaling molecules.¹¹¹ Towards more complex systems, by using urease-loaded alginate beads, a bistable switch was recently constructed that could respond from a low pH (unreacted “off”) state to a high pH (reacted “on”) state depending on the initial state of the beads.¹¹² However, the loading of urease in the alginate gel sphere proceeded with secondary gelation. First, the alginate bead was prepared by following the previously described method but with a short (60-second) crosslinking time. Then the premature alginate beads were placed in a concentrated urease solution to soak the urease overnight. In the next stage, the secondary gelation was performed with a freshly prepared CaCl_2 (6% w/v) solution for precisely 10 minutes at room temperature. This technique is helpful in creating desirable synthetic systems with new functions because it offers a straightforward way to entrap urease into an alginate gel network without changing its intrinsic kinetics.

In a more advanced way, a flow reactor device is currently employed to entrap enzymes non-covalently inside the hydrogel matrix. Recently, Prof. Bon and his research group reported independent responsive behavior and communication in

urease-immobilized alginate hydrogel fibers (Fig. 11) where they immobilized urease using a flow device.¹¹³ The device contained a glass capillary outlet with the desired configuration illustrated in Fig. 11 to allow a biphasic flow of the aqueous alginate phase and an inner flow of the oil phase. The output capillary of the device was pointed into a bath of aqueous calcium chloride solution (0.1 mol dm^{-3}). A vegetable oil phase containing 2 g L^{-1} of oil was pumped through a 0.1 g L^{-1} solution of sodium alginate of the desired urease concentration to form droplets of low-size dispersity. As a result, the biphasic flow promotes the formation of calcium-cross-linked sodium alginate hydrogel fibers to entrap the urease, which also contained the oil droplets.

The introduction of an environmental signal in the form of urea caused an increase in local pH through the action of urease, which was trapped in the alginate fiber. The increased pH allowed for the deprotonation of the surrounding preexisting EDTA (ethylenediaminetetraacetic acid), which in turn was capable of chelating Ca^{2+} from the alginate fiber networks. This led to the destruction of the alginate fibers, which released the oil droplets. Thus, the fabricated urease-immobilized hydrogel fibers could interact with time control in response to a trigger originating from their environment. This provided a level of autonomy and translated the information from the environment to the material itself, which behaves according to the local pH responses. The same group also demonstrated temporal and spatial programming in soft composite hydrogel objects by immobilizing urease in the alginate gel.¹¹⁴ To attain

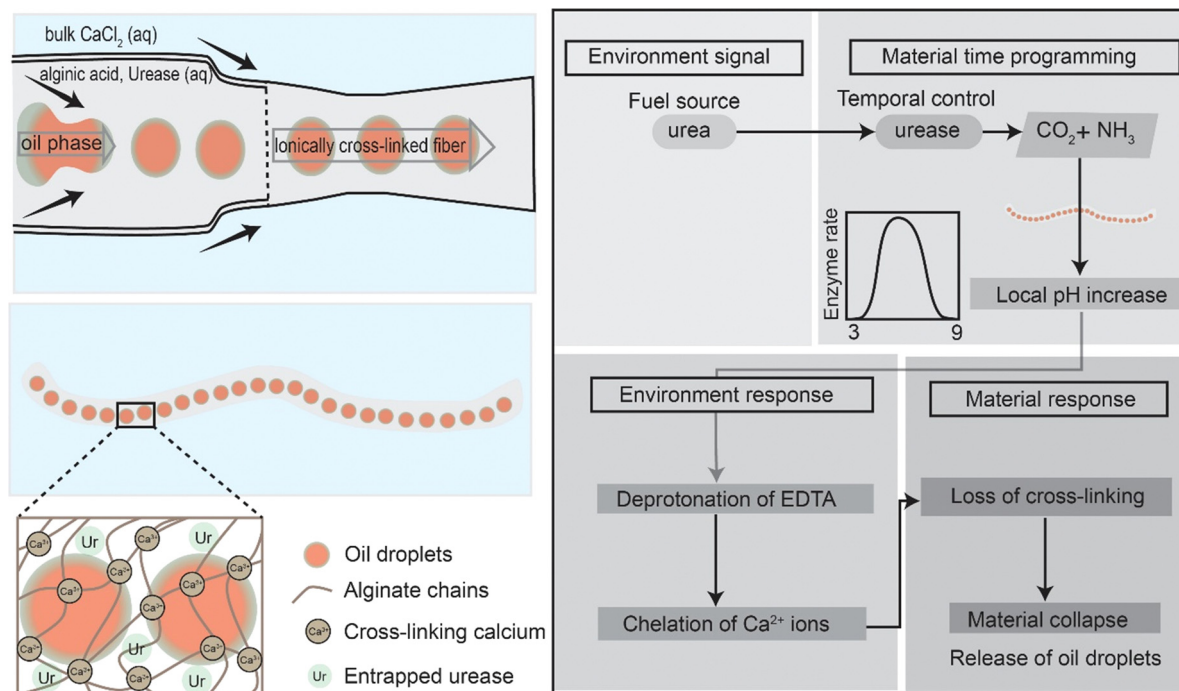


Fig. 11 Strategy of microfluidic synthesis of calcium-ion cross-linked sodium alginate fiber (left). Both the enzyme urease and oil droplets were entrapped in the alginate gel network. Urease-immobilized alginate gel structure shows responsive behavior by processing environmental signals into material responses (right). After a defined time period, the fiber results in an increase in pH by converting urea to ammonia. As the pH of the fiber increases locally, EDTA is deprotonated locally and chelates calcium ions which in turn results in a loss of cross-linking and the release of oil droplets. Adopted and reproduced under the terms of the CC-BY license, ref. 113, Copyright 2017, published by RSC.

the complex gel structure, a pre-gel mixture containing urease was loaded into the templates and exposed to a fine jet spray of calcium chloride solution (0.1 mol dm^{-3}) to induce ionic cross-linking of the alginate polymer chains by calcium ions.

Agarose is another promising biopolymer that was utilized to immobilize urease without altering its inherent kinetics as an alternative to alginate. Additionally, the agarose gel can provide the appropriate gel structures for particular purposes and design systems. To that end, using urease-loaded agarose beads, Taylor and her research team investigated reaction-induced convection toward comprehending quorum sensing.¹¹⁵ Urease-immobilized agarose beads were made using a straightforward but multi-step procedure. After being heated to $90 \text{ }^\circ\text{C}$, the agarose solution was progressively allowed to cool. The appropriate quantity of urease was added to the suspension once it had reached $50\text{--}55 \text{ }^\circ\text{C}$. The following step involved transferring 1 milliliter of the agarose and enzyme suspension mixture into a syringe. The syringe was then used to transfer the agarose and enzyme mixture drop by drop into a hexane bath. Urease was encapsulated within the agarose gel network and settled at the bottom of the hexane bath after the drop of agarose and urease mixture transformed into a gel bead in hexane. The beads were collected and given a water wash after half an hour. In the next step, the beads of the same size (2 mm) were used to conduct the quorum sensing experiment. Thus, this straightforward urease immobilization strategy has promise for the development of soft materials with a variety of uses. Additionally, Table 1 delineates multiple strategies for urease immobilization on diverse scaffolds and outlines several potential uses.

3. Urease-urea FCRN toward systems chemistry and materials sciences

Most of the biological events, such as metabolic function, transcription, translation, cellular memory, cellular communications, biological patterns and others, occur through a variety of feedback mechanisms.¹¹⁶ The key mechanism includes complex concatenated biological networks that operate through feedback modules resulting in non-linear outputs, including bi(multi)stability, oscillations, switchable states and memory functions. However, comprehending such an event experimentally presents the next level of challenge. In this context, systems chemistry offers the possibilities of studying and understanding such complex phenomena with small synthetic networks, including peptides, proteins, DNA–RNA, enzymes or other small molecular networks.^{16,18,117} Among these, urease-urea is one of the finest systems capable of yielding various non-linear properties. Urease catalyzes the hydrolysis of urea, yielding carbon dioxide and the base ammonia, increasing the system's pH. The most intriguing feature of such a small reaction system is its network topology, which is composed of a positive feedback and a coupled negative feedback—displaying a bell-shaped activity curve that physically signifies that the reaction rate likely progressively increases with increasing pH, which is controlled by the positive feedback, reaches a maximum at pH 7,

and once the pH goes beyond pH 8, the reaction self-diminishes by the inherent negative feedback. This feature is indeed a key requirement for creating systems with various nonlinear functions.

For instance, Taylor and co-workers reported bifurcation, bistability, pH wave fronts, and oscillations by employing the urease-urea FCRN under the quasi-open and open system reaction configuration.^{118,119} The homogeneous urease-urea FCRN can be coupled to other chemical or material systems to realize desired functions. Interestingly, the urease-urea autocatalytic reaction was shown to facilitate the event of pH front propagation with constant velocity to guide the polymerization and achieve the temporal control of gelation.¹²⁰ Furthermore, the homogeneous urease-urea FCRN was applied to regulate dynamic self-assembly for programming gelation and triggering the sol–gel and gel–gel transitions.^{121–124} Toward achieving a more complex system, this FCRN is coupled with another antagonistic chemical system in which one pathway increases the pH while others compete for lowering the pH. With this system configuration, an autonomous system can be prescribed, allowing a metastable transient state only if the two coupled opposite processes can be separated by their kinetic mismatch.¹²⁵ Such autonomous systems offer a broad scope of application, including temporal conformation control of proteins, i-motif switch of DNA, developing transient hydrogels with programmable lifetime, constructing mini-homeostatic supramolecular systems, and controlling co-assembly and self-sorting of the fibers in multicomponent gels.^{32,33,126–128} More interestingly, Prof. Adams and coworkers recently reported the forging of out-of-equilibrium supramolecular gels by employing a coupled urease-urea/glucono- δ -lactone (GdL) pH autonomous system.¹²⁹ Their work demonstrated a ‘forging’ approach in which shear force (external invasive) and magnetic field (non-invasive) were applied to rearrange the underlying *L,D*-2NapFF peptide (Nap: naphthalene, F: phenylalanine) network from random to aligned fibers where the system switches a pre-programmed gel-to-sol-to-gel state driven by the autonomous pH processes.

In the next approach, the diffusion chemistry is coupled with the urease-urea FCRN by immobilizing urease in various nano(micro) structures or macroscopic gel matrices, providing a heterogeneous reaction system which allows diffusion of educts between the compartmentalized reaction hub and the surrounding solvent. The interplay between the diffusion process and FCRN kinetics invokes many interesting functions, such as front propagation, damping, bistability, oscillation, long-range communications, viscoadaptive behavior with artificial cells and others.^{100,110–112,130} Recently, Prof. Walther and coworkers designed a urease/glucose oxidase (GO_x)-based pH autonomous system that programmes the volume changes of pH-sensitive polymeric microcapsules, which control the permeability and impermeability of the microcapsules to regulate the catalytic reaction. They constructed artificial cells (ACs) using enzyme-encapsulated polymeric microcapsules *via* microfluidics, utilizing a water–oil–water (w/o/w) double emulsion generated through a double cross-junction microfluidic device.

Table 1 Summary of the different methods for immobilizing urease on different scaffolds

S. no.	Methodology	Chemical/physical process	Scaffolds	Description/applications	Ref.
01.	Covalent	Amide coupling <i>via</i> EDC	Carboxylic acid functionalized phosphonate-grafted Fe ₃ O ₄ NPs	Enzymatic catalysis in biotechnological processes. Immobilized enzymes are implemented in degrading pollutants	56
02.	Covalent	Amide coupling <i>via</i> DCC	Amino-functional Fe ₃ O ₄ NPs	Immobilized enzyme was utilized for urea removal from water samples with a hydrolysis efficiency between 91.7 and 95.0%	57
03.	Covalent	Amine–acid coupling reaction	Urease coupled hydrogel (UCG)	Immobilized urease can be stored for a long time while preserving its activity and also UCG showed significant enhancement in activity against thermal degradation compared to free urease	58
04.	Covalent	Carbodiimide-coupling reaction	Enzyme electrode (urease/BSA-PPy/ITO)	A cost-effective and facile potentiometric biosensor has been made based on bovine serum albumin (BSA)-embedded surface-modified polypyrrole for the quantitative estimation of urea in aqueous solution	59
05.	Covalent	Amide linkage <i>via</i> EDC/NHS coupling	Carboxyl-functionalized 3D porous polypyrrole (PPy)-based material using PPy nanoparticles (NPs)	The urease-immobilized materials show enhanced stability and activity of the enzyme	60
06.	Covalent grafting method	Amide linkage <i>via</i> coupling reagent (EDC) and an NHS by covalent bond formation	Carboxyl-functionalized PES beads	The urease-immobilized beads exhibited good thermal stability and hemocompatibility, which had the potential to be applied in the field of urea removal from blood with satisfactory efficiency	61
07.	Covalent method	Amide linkage <i>via</i> carbodiimide-based coupling reaction	Semiconducting thiophene copolymer poly(3-hexylthiophene-co-3-thiopheneacetic acid)	A potentiometric urease biosensor is developed for quantification of urea concentrations in industrial processes or biological samples	62
08.	Covalent method	Amide linkage <i>via</i> <i>N,N</i> -diethylaminoethyl methacrylate (EGDMA) crosslinker through a NHS and amine coupling reaction	Amine functionalized PDEAEMA hybrid microgel	Understanding urease-urea feedback-controlled reactions and emerging behavior such as self-regulation and temporal control of catalysis. This system mimics a “breathing” phenomenon with a microgel system by regulating gel expansion–contraction events	64
09.	Covalent	Disulfide linkage <i>via</i> <i>trans</i> -thioesterification reaction	Thiolated agarose and sepharose gel beads	Urease has been effectively immobilized through covalent attachment to thiolated sepharose, utilizing a mixed disulfide derivative of sepharose. This innovative approach facilitates the continuous hydrolysis of urea by the immobilized urease, enhancing its catalytic efficiency and stability for practical applications	65
10.	Covalent	Disulfide bond <i>via</i> Ellman's reagent	Siloxane-layer-coated magnetic iron oxide (Fe ₃ O ₄) nanoparticles	Magnetically retrievable immobilized urease is potentially promising for biomedical and environmental applications, and this immobilization strategy improved the residual activity of urease	66
11.	Covalent	Schiff-base covalent immobilization using imine linkage by Biginelli/Hantzsch reactions	Magnetic micro- or nano-cellulose-dialdehydes (MCD/NCD)	Urease immobilization to the cellulose microcrystal can improve the catalytic activities and reusability with a retention of 75–80% activity after six cycles of use	67
12.	Covalent	Imine linkage <i>via</i> glutaraldehyde as the crosslinker	ZnO-encapsulated polyaniline grafted chitosan (ZnO-en/PANI-g-CHIT)	Immobilized urease is used for potentiometric sensing of urea. Such a system is foreseen as a promising candidate toward the development of soft robots due to the capacity of spatial and temporal responses against environmental stimuli	68
13.	Covalent	Imine linkage <i>via</i> glutaraldehyde-mediated linker through a physical process	Polysulphone membrane	The immobilized urease exhibited good storage and operational stability. Additionally, it is powerful in the development of enzymatic membrane reactors due to its high reusability	69
14.	Covalent	Imine linkage <i>via</i> glutaraldehyde solution	Amine-functionalized silica gel microparticle	This study demonstrated the application of the enzyme thermistor for the analysis of urea in urine samples	71
15.	Covalent	Imine linkage	Silk fibroin (SF) membrane	A SF membrane-based portable urea sensor was fabricated that monitors the urea concentration under flow conditions	72
16.	Covalent	Imine linkage using glutaraldehyde as a cross-linking agent	Cysteine-capped copper nanoparticles [CCNPs]	In this strategy, immobilization efficiency was increased. The possibility of reusability of the immobilized enzyme and increased thermal and pH stability allow for various applications	73
17.	Covalent	Crosslinking <i>via</i> a radical reaction mechanism	Divinyl benzene and tripropylene glycol dimethacrylate-based polymer	The activity of free urease and CLUNAs was studied by hydrolysis of substrate urea using a phenol–hypochlorite assay for the determination of ammonia. Urease catalyzes the hydrolysis of urea to ammonia and carbon dioxide	78

Table 1 (continued)

S. no.	Methodology	Chemical/physical process	Scaffolds	Description/applications	Ref.
18.	Covalent	Diazo coupling reaction	Silane-based solid support	In order to improve the catalytic activity and facilitate the hydrolysis of urea, urease is covalently immobilized on a silane solid support that has been anchored with an aromatic nitro functionality	79
19.	Covalent	Polymerization reaction by using epoxy-bearing monomer	Poly(2-hydroxyethyl methacrylate-glycidyl methacrylate)-based nanoparticles	A highly stable urea biosensor was prepared by using poly(HEMA-GMA) nanoparticles, which were used as a nano-carrier for the urease enzyme. Urease-immobilized nanoparticles were used as a biosensor for analyzing the serum sample	80
20.	Covalent	Schiff base reaction	Polydopamine nanocapsules (PDA NC)	Urease immobilized polydopamine nanocapsules (PDA NC) were achieved by the reaction between the amine group of urease and the catechol group of PDA <i>via</i> a Schiff base reaction for constructing nanomotors for intravesical therapy of bladder diseases	81
21.	Covalent	Azide-alkyne cycloaddition reaction	Urease-functionalized DNA microtubes	Urease-immobilized DNA-based microswimmers were constructed. These swimmers can self-propel in fluid by urease-urea reaction, showcasing their programmability. This system provides a foundational proof of principle for developing artificial enzyme-controlled motors at the nanoscale	82
22.	Non-covalent	Ionic interaction	Amino resin particles	In this work, the clock behavior of the urea-urease-H ⁺ reaction with resin-immobilized urease was investigated	83
23.	Non-covalent	Electrostatic interaction	ZnO-nanowire arrays	A urea biosensor was constructed that retained its enzymatic activity due to the strong electrostatic interaction between zinc oxide and urease. Urease-immobilized ZnO nanowire electrode was also applied for selective determination of urea	86
24.	Non-covalent	Physical entrapment by electrostatic interaction occurring through conversion of the imidazole moiety into the imidazolium ion	Proton-conducting polymer networks of PAA with various compositions of PVI	Urease was successfully immobilized in a poly(1-vinyl imidazole) with poly(acrylic acid) (PAA/PVI) polymer network for investigating the proton conductivity of the system. Interestingly, the stability of immobilized urease towards temperature and pH, and its reusability and storage stability were enhanced by its entrapment	84
25.	Non-covalent	Biomimetic mineralization <i>via</i> ionic interaction	Zeolite imidazolate-based framework-8 (ZIF-8)	Biomimetic mineralization strategy was employed to achieve the immobilization of urease in a type of metal-organic framework. Urease@ ZIF-8 exhibited good recyclability during the degradation of urea	87
26.	Non-covalent	DNA-urease conjugation <i>via</i> hydrogen bonding and other physical interactions	Streptavidin coated magnetic beads	Urease-immobilized magnetic beads were used in the detection of DNA amplicons of polymerase chain reaction. This system was applied in a quantitative real-time PCR (qPCR) platform that targets specific genes associated with virulence, namely <i>tcdB</i> , <i>tcdC</i> , and <i>cdtB</i> . These genes are crucial as they encode for toxins and regulatory proteins that contribute to the pathogenicity of hypervirulent strains	85
27.	Non-covalent	Hydrogen bonding interaction	Polydimethylsiloxane (PDMS) sheet	The immobilized nanometer-sized enzyme molecules can effectively propel centimeter-scale sheets in solution, as shown by experiments and modeling. This propulsion is facilitated through chemo-mechanical transduction, where the surrounding fluid plays a crucial role in connecting the nano-scale enzymatic activity to macro-scale motion	88
28.	Non-covalent	Encapsulation technique (physical process)	Nanovesicles	Urease-immobilized mesoscopic compartments were used to underscore the collective behavior of urease pH clocks in nano- and microvesicles and control the event of fast ammonia transport	95
29.	Non-covalent	Electrostatic interactions	Block copolymer based polymersome nanoreactors	A self-adaptive polymersome nanoreactor has been developed by immobilizing urease and other enzymes in the polymersome that drives many catalytic reactions out of equilibrium by controlling the permeability of its membranes over time	97
30.	Non-covalent	Hydrophobic interactions	Block copolymer of mPEG ₄₅ - <i>b</i> -p[DEAEMA ₁₇₅ - <i>g</i> -BMA ₂₈]	Urease was immobilized in bicontinuous nanospheres (BCNs), which were applied to achieve the self-regulation of the system's pH and membrane permeability by utilizing a urease-urea feedback reaction	98
31.	Non-covalent	Ionic interactions	Poly(ethylene glycol)- <i>b</i> -(poly(butyl acrylate)- <i>co</i> -poly(penta fluorophenyl acrylate)) (PEG- <i>b</i> -PHPMA) hydrogel based nanoreactors	The enzyme-immobilized nanocompartments were used to demonstrate the photo-switchable gating of a non-equilibrium enzymatic feedback system and mimic chemical communication among the polymersome nanoreactors, in a manner similar to that of cellular biology	99

Table 1 (continued)

S. no.	Methodology	Chemical/physical process	Scaffolds	Description/applications	Ref.
32.	Non-covalent	Ionic interactions and hydrogen bonding	DNA-based protocell	Urease-based reactions inside the urease-immobilized DNA-based protocell allowed for the transportation of protocell logistics, such as cell-like transporter systems, and followed an oscillatory mechanism for repeated pick-up and delivery of molecular cargo	100
33.	Non-covalent	Ionic interactions	pH responsive capsules (urea@H-SiO ₂ @PE) with hollow silica core and microgel	Life-like functions were addressed, such as programmable interactive communications and self-regulation behaviors by urease immobilized materials occurring through a feedback-controlled reaction mechanism. These systems mimic biological processes, allowing for dynamic responses to environmental stimuli	101
34.	Non-covalent	Entrapment method	Acrylamide copolymer-based hydrogels	The urease coupling allowed for optimizing the structure and properties of thermo-responsive hydrogels composed of semi-interpenetrating polymer networks (SIPNs). This approach aimed to enhance the strength, modulus, and swelling–shrinking deformation of the hydrogels	102
35.	Non-covalent	Entrapment by photopolymerized polymer hydrogel	Polymer hydrogel	This system enables layered compartments containing antagonistic pH-modulating enzymes to design acidic and alkaline pH lifecycles and facilitate transient pH signals in a supernatant solution. The pH-flips technique was combined with peptides to provide hydrogel material systems and time-programmed self-assemblies	104
36.	Non-covalent	Entrapment inside the polymer hydrogel	Poly aspartic acid <i>N</i> -acrylamide (A3)-based hydrogel	Responsive soft robots were developed by immobilizing urease in the polymer gel blocks. The soft robot exhibited homeostatic-like autonomous activities driven by chemo-mechanical feedback mechanisms, particularly monitoring by urease-urea chemical reaction networks	105
37.	Non-covalent	Physical entrapment	Hydrogels based on poly(acrylic acid-co-dimethylaminoethyl methacrylate)	Urease-immobilized polymer hydrogel was employed to design a piezoresistive hydrogel biosensor for the detection of urea	106
38.	Non-covalent	Emulsion polymerization	Thiol-poly(ethylene glycol) acrylate (PEGDA) hydrogel beads	Urease-immobilized polymer beads were effectively used to investigate the pH clock and other non-linear responses. The enzyme immobilization allowed significant enhancement of enzyme stability from hours to days under the tested conditions	107
39.	Non-covalent	Physical entrapment	Ca ²⁺ cross-linked alginate hydrogel	The feedback reaction network with a solely urease-urease system or with a coupled network of esterase was investigated in a heterogeneous system driven by a compartmentalized reaction hub to comprehend the various possibilities of non-linear functions. The pH front and reaction diffusion chemistry are utilized to realize the artificial membrane activity and inter-sphere communication and further were applied to print various 2D/3D hydrogel structures	110
40.	Non-covalent	Ionic interactions	Alginate beads	Urease-immobilized millimetre-sized, soft hydrogel beads provide a suitable platform to comprehend the chemical communication, which will be helpful to understand cellular signal processing	111
41.	Non-covalent	Entrapment method	Soft hydrogel alginate-based fibers and beads	This technology has the ability to program a self-regulated pH shift, which triggers the intended reaction of gel fibre disintegration or a colour shift in gel beads. The urease-entrapped system enables inter-material communication on shorter length scales and the autonomous response behaviour of a group of bodies in a single closed system	113
42.	Non-covalent	Ionic interactions	Hydrogel	A simple gelation procedure creates urease-entrapped soft composite hydrogel objects and oil droplets for a time- and space-programmable autonomous process. In response to urea, these continuous objects with non-uniform dimensional composition change colour or dissolve at specified hydrogel structure locations at predetermined time intervals. These hydrogels' spatial and temporal reactions to environmental stimuli make them useful instruments for applications like soft robotics	114

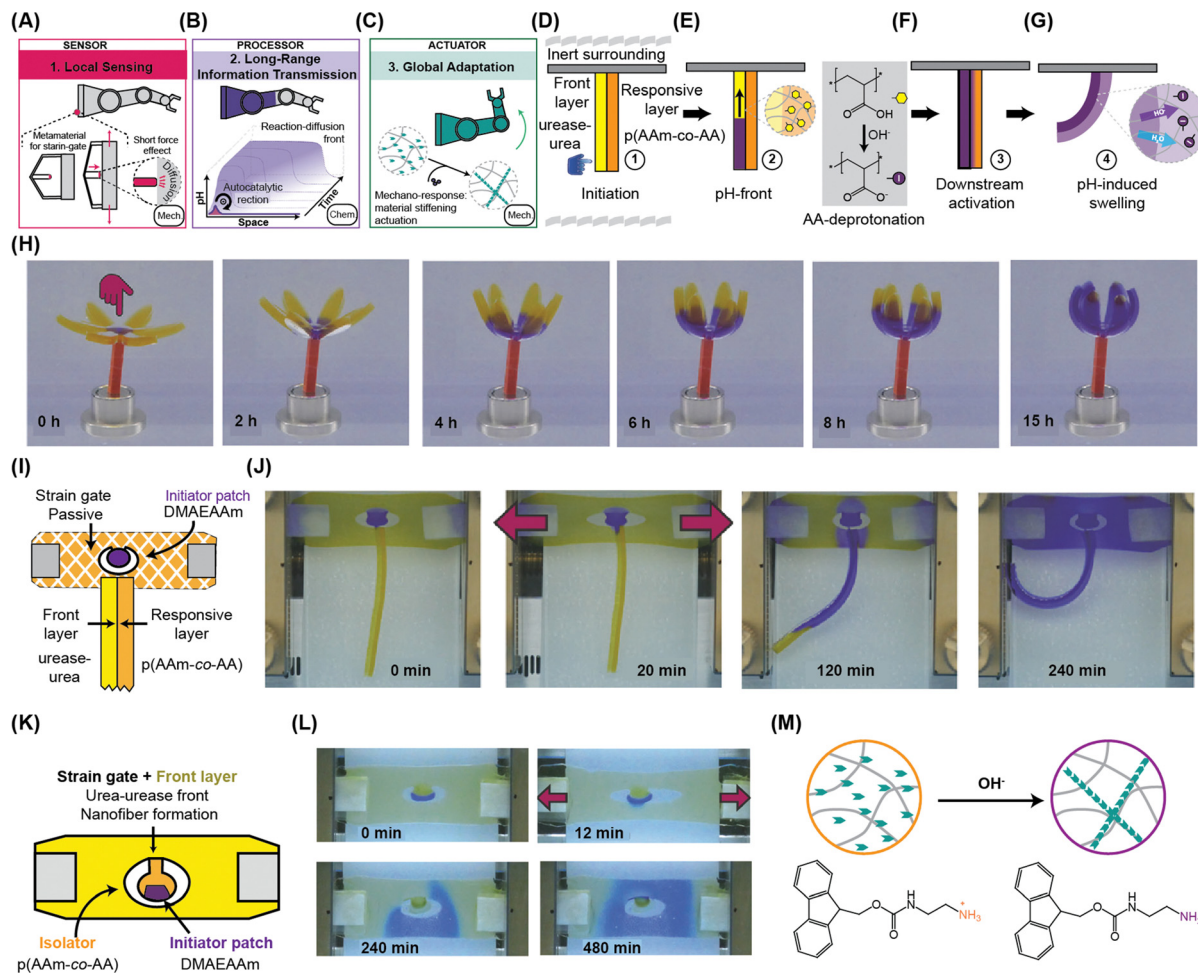


Fig. 12 (A)–(C) Design concept of the adaptive hydrogel-based sensor–processor–actuator model involving chemo-mechanical and local to global information processing. (D)–(G) Operational steps to drive bilayer actuators involving (D) starting dormant state before the soft touching, (E) OH^- -autocatalytic front propagation in the front layer, (F) OH^- diffusion from the front layer to the connected pH sensitive responsive layer, and (G) bending due to the swelling of the responsive layer. (H) Self-protective process in a bilayer flower (bottom: responsive, top: front layer). Each layer is initially 0.75 mm thick. (I) Scheme of the remotely activated soft robotic bilayer by using metamaterial strain gates and chemical information-processing. (J) Real-time images of the strain-gated soft robot bending with a remote metamaterial sensor. (K) Scheme of the device to achieve the strain-gated global mechano-adaptation due to nanofiber self-reinforcement after the desired touching. (L) Time-lapse images of the spreading of OH^- front in the strain-gated meta-gel. (M) OH^- -induced self-assembly of nanofibrils of Fmoc-ethylenediamine hydrochloride inside the hydrogel. (Note: Aam, acrylamide; AA, acrylic acid; DMAEAAM, *N*-[2-(dimethylamino)ethyl]acrylamide.) Adopted and reproduced under the terms of the CC-BY license, ref. 132, Copyright 2024, published by Springer Nature.

Interestingly, the pH modulation capabilities driven by the autonomous systems enable homeostatic and collective self-protection behavior in artificial cell-like spheroids.¹³¹ Furthermore, the same group recently immobilized urease-urea reaction in a polymeric bilayer gel system and engineered the mechano-adaptive meta-gels through synergistic chemical and physical information processing (Fig. 12).¹³² They have demonstrated a platform that combines metamaterial unit cells with a pH-autocatalytic urease-urea FCRN to create a sensor–processor–actuator system for mechanical materials and soft robotics (Fig. 12(A)–(C)). Toward constructing the next generation of functional devices in sensor–processor–actuator material systems, they demonstrated a touch-active autonomous actuator by combining sPEG-urea-urease (sPEG, star-shaped polyethylene glycols) pH front layers with pH-sensitive response layers.

A combination of acrylamide (AAm, passive), acrylic acid (AA, pH-sensitive), and a cross-linker was used to photo-polymerize the response layer. The device's mechanism is demonstrated in Fig. 12(D)–(G), where a touch of a high-pH hydrogel piece (Fig. 12(D)) permits a catalytic amount of OH^- to diffuse into the front layer and initiates the front propagation through autocatalytic OH^- amplification (Fig. 12(E)). This trigger activates the downstream processes *via* deprotonation of the AA moieties (Fig. 12(F)). Simultaneously, the reaction diffusion (RD) front layer contracts and the bilayer flexes as a mechanical downstream process (Fig. 12(G)). Subsequently, this proof of concept effectively illustrated a self-protecting flower, wherein the petals were constructed from a horizontally orientated 2D bilayer, with an RD front layer over a response layer beneath (Fig. 12(H)). They next built a strain-gated remote initiation of a

soft robotic actuator by combining the metamaterial strain gate with a hydrogel bilayer (Fig. 12(I) and (J)). Only strain-gated soft touching, as shown in Fig. 12(I), allows the OH^- ions to diffuse slowly to the connecting bilayer in this high pH (pH 10) patch constructed of a cross-linked p(AAm-co-DMAEAAm) hydrogel. The remaining strain gate (pH = 2.75) was composed of cross-linked pAAm with urea, a BCP indicator, and was urease-free. To activate the bilayer device, they stretched the module to the touching point. After the initiation event occurred, the touching was eliminated. Notably, the self-sustaining RD front advanced along the bilayer, subsequently enabling localized bending as the front continued its propagation until complete bending was achieved (Fig. 12(J)). The same concept was utilized for strain-gated adaptation towards mechanical strengthening by downstream self-assembly of nanofibers in the main body of a meta-gel (Fig. 12(K)–(M)). In their design, the main body contained Fmoc-ethylenediamine hydrochloride (Fmoc-EDA), which is prone to assemble into nanofibers above pH 8.4 (Fig. 12(K) and (L)). Upon applying suitable tension, the RD front is initiated, and the OH^- signal propagates through the material to facilitate the self-assembly of Fmoc-EDA into nanofibers (Fig. 12(L) and (M)). This downstream regulatory actuator strengthens the mechanical properties of the whole metamaterial based on the local touching event. Thus, urease-urea FCRN serves as a promising module to comprehend the complex systems biology events in synthetic approaches and has propelled the advancement of systems chemistry and soft materials to realize system-level applications.

4. Characterization of urease immobilization

This review highlights several methods, encompassing both covalent and non-covalent strategies, employed for the immobilization of urease on various scaffolds. Nonetheless, each immobilization method requires particular reaction conditions and system configurations. A key inquiry pertains to the techniques for verifying the immobilization of urease onto various scaffolds. In pursuit of this objective, a range of characterization techniques, including urease activity assay tests, UV-Vis spectroscopy, fluorescence spectroscopy, X-ray diffraction, XPS data, FTIR spectroscopy, scanning electron microscopy (SEM), and transmission electron microscopy (TEM), are commonly employed to validate the immobilization of urease.^{56,58,133} The immobilized urease is characterized by comparing the degree of crystallinity or amorphous nature of the pristine substrate with that of the urease-immobilized substrate using an X-ray diffractometer and by examining the size and shape of the substrates prior to and following urease immobilization using a variety of microscopic techniques, including SEM and TEM.⁵⁷ Moreover, urease immobilization on different scaffolds is confirmed by FTIR spectroscopy, which offers more concrete proof of identifying particular functional groups of the urease enzyme.¹³⁴ More specifically, several types of fluorophore labeling are often used in techniques to describe

the covalent and non-covalent urease immobilization to the DNA-based conjugates, supramolecular nanostructures, or hydrogels.^{82,85,110} This procedure involves labeling urease with a particular fluorophore and immobilizing it on the scaffolds. The immobilization of urease is then confirmed by fluorescence spectroscopy, microscopy, and confocal laser scanning microscopy (CLSM). Apart from the aforementioned characterization techniques, other tools such as X-ray photoelectron spectroscopy (XPS), thermogravimetric analysis (TGA), circular dichroism (CD) spectroscopy, atomic force microscopy (AFM), time-of-flight secondary ion mass spectroscopy (TOF-SIMS), opto-chemical sensing, and sum frequency generation (SFG) spectroscopy are also currently employed for the characterization of immobilized urease and other enzymes. XPS gives a complete analysis of elements, helping to closely examine surface layers post-immobilization. It provides information about chemical states and elemental composition, improving the understanding of their structure and chemical properties. This, in turn, makes immobilization methods more effective in different industrial and research uses.^{135,136} Thermogravimetric analysis (TGA) is also a technique that allows for the determination of the thermal stability and the degree of functionalization of the support material post-immobilization. It provides information on the thermal properties of the immobilized enzyme (urease) systems by measuring weight variations as a function of temperature.¹³⁵ Furthermore, CD spectroscopy is indeed helpful in characterizing enzyme immobilization including urease, by providing structural information with reference to protein–ligand interactions and protein–protein interactions, structural compositions of proteins, and kinetic and thermodynamic information about macromolecules.¹³⁷ Another potent method for comprehending the distribution of enzymes on surfaces at the submicron scale is TOF-SIMS, which provides thorough chemical mapping and may successfully disclose the chemical structure of the surface of immobilized enzymes as well as information on their orientation.¹³⁵ In addition, opto-chemical sensing allows for the assessment of the internal environment of immobilized enzymes, providing insights into how different conditions affect enzyme activity within porous supports.¹³⁶ Sum frequency generation (SFG) spectroscopy is another important optical technique that is useful for analyzing surface-bound enzymes, including urease.¹³⁸ Furthermore, the degree of functionalization can be accurately determined using Nessler's technique and the urease activity assay.^{56–58,83} Although many tools can offer valuable insights into determining enzyme (urease) immobilization on various surfaces, their practical application can be constrained by their inherent complexities and cost factors. Therefore, determining the degree of urease functionalization to the different scaffolds is quite difficult.

5. Selection of immobilization strategies for the targeted functions

In this study, we thoroughly describe the several approaches to urease immobilization that can be used to build different

chemical and material systems that have a range of uses. It does, however, require a basic guideline for choosing the precise immobilization techniques that must be used for on-demand tasks. In this regard, covalent urease immobilization is a tricky process. It requires complex chemical synthesis, which is sometimes a difficult and time-consuming process. However, it can offer more advantages in a range of sensing-oriented applications because urease is permanently immobilized to the scaffolds.³⁸ In order to facilitate multiple usages of the urease-immobilized devices and reduce the effective cost of a sensor in therapeutic and biotechnical applications, covalent immobilization is a preferred and widely used methodology. Not only for the above-mentioned reason, but sometimes an unfavorable system configuration prevents urease from being trapped on the hard surface of nano(micro)particles or other scaffolds. For instance, the absence of urease-hosting spaces in glass surfaces, carbon compounds, metal nanoparticles, and microparticles precludes non-covalent immobilization.^{24,25,31,34,38} Moreover, these scaffolds do not contain intertwined three-dimensional networks, which can entrap the urease. In this context, chemical reaction-mediated urease immobilization is the only alternative in which the surface of respective scaffolds is firstly modified with a suitable functional group, and then urease immobilization is performed with specific chemical reactions. The availability of the functional group on the scaffold surface primarily determines the choice of chemical reactions. Specifically, if the system required dynamic operation, urease is then attached to the scaffolds by dynamic linkage through reversible disulfide or imine bonds. Otherwise, more stable amide coupling, diazo coupling, radical polymerization, and other techniques are employed.

On the contrary, non-covalent urease immobilization is preferable for systems chemists in developing new systems and materials that possess features similar to those of living systems.^{13,19} Importantly, the counter-ionic attraction forces and hydrogen bonding play an additional role in making the urease confinement under the polymer-based soft nanostructures or soft materials more feasible.^{45,46,49} The non-covalent urease entrapment inside the micro(nano)compartments, 3D-gel scaffolds, and others provides a benefit in introducing heterogeneity into systems where the physical process of reaction diffusion could be coupled with the feedback-controlled reaction network. The interplay between the urease reaction network and the reaction diffusion could invoke the required functions. More particularly, the whole system configuration achieved by non-covalent urease immobilization inside the soft materials is competent toward the construction of smart adaptive soft materials with animate-like functions. Stepping to the next level, non-covalently immobilized urease-based soft material devices have potential for next-generation soft robots.⁶¹ Therefore, non-covalently immobilized urease systems under the soft compartment can add parallel diffusion events, whose kinetics also play a significant role in capturing heterogenic spatiotemporal phenomena.⁶⁵ Besides these advantages, the non-covalent immobilization technique is also straightforward to handle and less time-consuming. If the demanded functions

are met with non-covalent urease immobilization, one can easily bypass the complexity of chemical reaction-mediated immobilization. On the other hand, covalent immobilization to the surface of the scaffolds could not shield the reaction center, which is directly exposed to the surrounding environment and, therefore, is lacking in coupling the diffusion chemistry with feedback reaction systems. Therefore, the choice of enzyme immobilization strategies is one of the instrumental factors to reach the desired systems and functions, which is briefly discussed throughout the review.

6. Conclusion and outlook

Despite various advantages of the homogeneous urease-urea FCRN, such as inducing pH-responsive gelation, controlling hydrogel properties, tuning nanoparticle properties, developing autonomous chemical and material systems, and regulating the folding of proteins, peptides, and DNA, the strategy faces several challenges.¹⁹ First, FCRN's activity is restricted to the pH 3–9 range; after that, it ceases to be active. Another significant problem is that over the course of several system cycles, the urease gradually loses its activity in solution. Furthermore, the homogeneous urease-urea FCRN can be significantly impacted by temperature fluctuations as well as ambient oxygen and carbon dioxide levels, leading to challenges with reproducibility.¹³⁹ These drawbacks can be addressed to some extent while urease is immobilized to the solid support.

Therefore, this review includes a concrete demonstration of various strategies available for urease immobilization. Chemical bond formation or non-covalent interactions are the master tools to achieve urease immobilization on specific substrates. It is noteworthy that the solvent-exposed functional groups of urease, including $-\text{NH}_2$, $-\text{COOH}$, $-\text{SH}$, $-\text{OH}$, and charged side chains of amino acid sequences, have a wide range of reactions and physical interactions that allow them to immobilize a variety of scaffolds, including solid surfaces, nano(micro)particles, microgels, hydrogels, and supramolecular nanoarchitectures. Urease immobilization not only facilitates easy accessibility and reusability, but it also provides the capacity for long-term storage with intact function and averts its degradation under harsh pH and temperature cues.¹⁴⁰ In addition, a suitable substrate could offer extra support to maintain the structural integrity of enzymes by stabilizing the multimeric subunits of proteins.¹⁴¹ All these advantages are governed by the immobilized urease enzyme, which expands its applications in many areas, including the development of efficient biocatalysts, biosensors, and therapeutics.

Urease immobilization, however, faces a number of challenges. When urease is immobilized, it often undergoes significant conformational changes that reduce its catalytic activity. More specifically, the local lower pH environment kills the urease irreversibly when it is immobilized in the polymeric networks containing acidic or highly basic functional groups. One of the biggest challenges in urease immobilization is

maintaining its reactivity when it demands reversible immobilization employing thiol–disulfide or imine chemistry, or in the radical-rich environment. However, these issues could be effectively resolved by applying suitable environmental conditions and experimental configuration.

Nevertheless, the compartmentalized urease-urea reaction hub effectively integrates reaction-diffusion chemistry, presenting significant opportunities for developing novel chemical and material systems that exhibit life-like functions such as self-regulation, chemical morphogenesis, spatiotemporal self-organization, communication, and memory capabilities.^{18,26} The immobilized urease showcases precise programmability and controllability in its reaction kinetics. Therefore, coupling the compartmentalized urease reactions with soft materials that could respond to pH changes would facilitate the development of soft robots. Taking the complexity to the next level, the ability to generate motion in immobilized urease machines would allow for the development of self-propelled macroscale machines that could serve various biological applications. In the real world, compartmentalized feedback reaction networks operated by immobilized urease will be instrumental in the facile development of next-generation life-like material systems. Thereby, exciting developments can be foreseen beyond the present-day proof-of-concept.

Author contributions

S. H. and V. A. R. prepared the figures. S. H., V. A. R. and I. M. reviewed the literature, analyzed the data, and wrote the manuscript.

Data availability

No primary research results, software or code have been included, and no new data were generated or analyzed as part of this review.

Conflicts of interest

The authors declare no competing interests.

Acknowledgements

I. M. acknowledges the financial support by Jain University (JU/ MRP/CNMS/27/2022) and the ANRF SURE research grant (SUR/2022/004646).

References

- S. M. Cuesta, S. A. Rahman, N. Furnham and J. M. Thornton, *Biophys. J.*, 2015, **109**, 1082–1086.
- P. K. Agarwal, *Microb. Cell Fact.*, 2006, **5**, 2.
- J. G. Robertson, *Curr. Opin. Struct. Biol.*, 2007, **17**, 674–679.
- J. L. Adrio and A. L. Demain, *Biomolecules*, 2014, **4**, 117–139.
- D. Cowan, *Trends Biotechnol.*, 1996, **14**, 177–178.
- P. M. Nielsen, *Enzymes in Food Technology*, 2009, pp. 292–319, DOI: [10.1002/9781444309935.ch13](https://doi.org/10.1002/9781444309935.ch13).
- M. van Oort, *Enzymes in Food Technology*, 2009, pp. 1–17, DOI: [10.1002/9781444309935.ch1](https://doi.org/10.1002/9781444309935.ch1).
- M. Orbán, K. Kurin-Csörgei and I. R. Epstein, *Acc. Chem. Res.*, 2015, **48**, 593–601.
- N. E. Dixon, C. Gazzola, R. L. Blakeley and B. Zerner, *J. Am. Chem. Soc.*, 1975, **97**, 4131–4133.
- B. Krajewska, *J. Mol. Catal. B: Enzym.*, 2009, **59**, 9–21.
- K. Stingl, K. Altendorf and E. P. Bakker, *Trends Microbiol.*, 2002, **10**, 70–74.
- E. M. Brookes and D. A. Power, *Sci. Rep.*, 2022, **12**, 20827.
- S. Tischer, M. Börnhorst, J. Amsler, G. Schoch and O. Deutschmann, *Phys. Chem. Chem. Phys.*, 2019, **21**, 16785–16797.
- C. Follmer, *J. Clin. Pathol.*, 2010, **63**, 424.
- C. Rechenmacher, B. Wiebke-Strohm, L. A. Oliveira-Busatto, J. C. Polacco, C. R. Carlini and M. H. Bodanese-Zanettini, *Genet. Mol. Biol.*, 2017, **40**, 209–216.
- G. Ashkenasy, T. M. Hermans, S. Otto and A. F. Taylor, *Chem. Soc. Rev.*, 2017, **46**, 2543–2554.
- R. Merindol and A. Walther, *Chem. Soc. Rev.*, 2017, **46**, 5588–5619.
- H. W. H. van Roekel, B. J. H. M. Rosier, L. H. H. Meijer, P. A. J. Hilbers, A. J. Markvoort, W. T. S. Huck and T. F. A. de Greef, *Chem. Soc. Rev.*, 2015, **44**, 7465–7483.
- C. Sharma, I. Maity and A. Walther, *Chem. Commun.*, 2023, **59**, 1125–1144.
- M. G. Howlett, A. H. J. Engwerda, R. J. H. Scanes and S. P. Fletcher, *Nat. Chem.*, 2022, **14**, 805–810.
- S. N. Semenov, A. S. Y. Wong, R. M. van der Made, S. G. J. Postma, J. Groen, H. W. H. van Roekel, T. F. A. de Greef and W. T. S. Huck, *Nat. Chem.*, 2015, **7**, 160–165.
- A. Joesaar, S. Yang, B. Bögels, A. van der Linden, P. Pieters, B. V. V. S. P. Kumar, N. Dalchau, A. Phillips, S. Mann and T. F. A. de Greef, *Nat. Nanotechnol.*, 2019, **14**, 369–378.
- I. Maity, D. Dev, R. Cohen-Luria, N. Wagner and G. Ashkenasy, *Chem.*, 2024, **10**, 1132–1146.
- I. Maity, N. Wagner, R. Mukherjee, D. Dev, E. Peacock-Lopez, R. Cohen-Luria and G. Ashkenasy, *Nat. Commun.*, 2019, **10**, 4636.
- S. P. Afrose, S. Bal, A. Chatterjee, K. Das and D. Das, *Angew. Chem., Int. Ed.*, 2019, **58**, 15783–15787.
- V. A. Ranganath and I. Maity, *Angew. Chem., Int. Ed.*, 2024, **63**, e202318134.
- R. R. Mahato, P. E. Shandilya and S. Maiti, *Chem. Sci.*, 2022, **13**, 8557–8566.
- N. Wagner, R. Mukherjee, I. Maity, S. Kraun and G. Ashkenasy, *ChemSystemsChem*, 2020, **2**, e1900048.
- K. Kovacs, R. E. McIlwaine, S. K. Scott and A. F. Taylor, *J. Phys. Chem. A*, 2007, **111**, 549–551.
- L. Heinen, T. Heuser, A. Steinschulte and A. Walther, *Nano Lett.*, 2017, **17**, 4989–4995.
- T. Heuser, R. Merindol, S. Loescher, A. Klaus and A. Walther, *Adv. Mater.*, 2017, **29**, 1606842.
- L. Heinen and A. Walther, *Chem. Sci.*, 2017, **8**, 4100–4107.
- T. Heuser, E. Weyandt and A. Walther, *Angew. Chem., Int. Ed.*, 2015, **54**, 13258–13262.

- 34 A. S. Zadorin, Y. Rondelez, G. Gines, V. Dilhas, G. Urtel, A. Zambrano, J.-C. Galas and A. Estevez-Torres, *Nat. Chem.*, 2017, **9**, 990–996.
- 35 J. Wu, X. Wang, Q. Wang, Z. Lou, S. Li, Y. Zhu, L. Qin and H. Wei, *Chem. Soc. Rev.*, 2019, **48**, 1004–1076.
- 36 Y. Wu, L. Jiao, X. Luo, W. Xu, X. Wei, H. Wang, H. Yan, W. Gu, B. Z. Xu, D. Du, Y. Lin and C. Zhu, *Small*, 2019, **15**, 1903108.
- 37 A. Rodriguez-Abetxuko, D. Sánchez-deAlcázar, P. Muñumer and A. Beloqui, *Front. Bioeng. Biotechnol.*, 2020, **8**, 830.
- 38 A. Hussain, H. Rafeeq, N. Afsheen, Z. Jabeen, M. Bilal and H. M. N. Iqbal, *Catal. Lett.*, 2022, **152**, 414–437.
- 39 J. Meena, A. Gupta, R. Ahuja, M. Singh and A. K. Panda, *J. Mol. Liq.*, 2021, **338**, 116602.
- 40 J. Zdarta, A. S. Meyer, T. Jesionowski and M. Pinelo, *Catalysts*, 2018, **8**, 92.
- 41 C.-Y. Zhu, F.-L. Li, Y.-W. Zhang, R. K. Gupta, S. K. S. Patel and J.-K. Lee, *Polymers*, 2022, **14**, 1409.
- 42 M. Bisht, S. K. Thayallath, P. Bharadwaj, G. Franklin and D. Mondal, *Green Chem.*, 2023, **25**, 4591–4624.
- 43 M. Bilal, M. Asgher, R. Parra-Saldivar, H. Hu, W. Wang, X. Zhang and H. M. N. Iqbal, A review, *Sci. Total Environ.*, 2017, **576**, 646–659.
- 44 A. Basso and S. Serban, A review, *Mol. Catal.*, 2019, **479**, 110607.
- 45 P. Bharmoria, A. A. Tietze, D. Mondal, T. S. Kang, A. Kumar and M. G. Freire, *Chem. Rev.*, 2024, **124**, 3037–3084.
- 46 R. T. Ayinla, M. Shiri, B. Song, M. Gangishetty and K. Wang, *Mater. Chem. Front.*, 2023, **7**, 3524–3542.
- 47 E. R. Johnson, S. Keinan, P. Mori-Sánchez, J. Contreras-García, A. J. Cohen and W. Yang, *J. Am. Chem. Soc.*, 2010, **132**, 6498–6506.
- 48 S. Samanta, P. Raval, G. N. Manjunatha Reddy and D. Chaudhuri, *ACS Cent. Sci.*, 2021, **7**, 1391–1399.
- 49 I. Maity, D. B. Rasale and A. K. Das, *RSC Adv.*, 2013, **3**, 6395–6400.
- 50 A. K. Das, I. Maity, H. S. Parmar, T. O. McDonald and M. Konda, *Biomacromolecules*, 2015, **16**, 1157–1168.
- 51 I. Maity, D. B. Rasale and A. K. Das, *Soft Matter*, 2012, **8**, 5301–5308.
- 52 I. Maity, D. Dev, K. Basu, N. Wagner and G. Ashkenasy, *Angew. Chem., Int. Ed.*, 2021, **60**, 4512–4517.
- 53 C. Ghosh, S. Menon, S. Bal, S. Goswami, J. Mondal and D. Das, *Nano Lett.*, 2023, **23**, 5828–5835.
- 54 D. Procopio, C. Siciliano and M. L. Di Gioia, *Org. Biomol. Chem.*, 2024, **22**, 1400–1408.
- 55 S. Chen and J. Xu, *Tetrahedron Lett.*, 1991, **32**, 6711–6714.
- 56 B. Sahoo, S. K. Sahu and P. Pramanik, *J. Mol. Catal. B: Enzym.*, 2011, **69**, 95–102.
- 57 S. R. Hormozi Jangi, M. Akhond and Z. Dehghani, *Process Biochem.*, 2020, **90**, 102–112.
- 58 S. N. R. Kutcherlapati, N. Yeole and T. Jana, *J. Colloid Interface Sci.*, 2016, **463**, 164–172.
- 59 T. Ahuja, I. A. Mir, D. Kumar and Rajesh, *Sens. Actuators, B*, 2008, **134**, 140–145.
- 60 E. M. Kutorglo, F. Muzika, F. Hassouna, G. Storti, D. Kopecký, R. Bleha, A. Synytsya, I. Sedlářová and M. Šoóš, *Microporous Mesoporous Mater.*, 2021, **311**, 110690.
- 61 J. Zhang, Z. Wang, C. He, X. Liu, W. Zhao, S. Sun and C. Zhao, *ACS Omega*, 2019, **4**, 2853–2862.
- 62 C.-Y. Lai, P. J. S. Foot, J. W. Brown and P. Spearman, *Biosensors*, 2017, **7**, 13.
- 63 M. Urbanowicz, K. Sadowska, A. Paziewska-Nowak, A. Soldatowska and D. G. Pijanowska, *Membranes*, 2021, **11**, 898.
- 64 H. Che, B. C. Buddingh and J. C. M. van Hest, *Angew. Chem., Int. Ed.*, 2017, **56**, 12581–12585.
- 65 J. Carlsson, R. Axén, K. Brocklehurst and E. M. Crook, *Eur. J. Biochem.*, 1974, **44**, 189–194.
- 66 R. P. Pogorilyi, I. V. Melnyk, Y. L. Zub, G. A. Seisenbaeva and V. G. Kessler, *J. Mater. Chem. B*, 2014, **2**, 2694–2702.
- 67 F. Tamaddon, D. Arab and E. Ahmadi-AhmadAbadi, *Carbohydr. Polym.*, 2020, **229**, 115471.
- 68 C. S. Kushwaha, P. Singh, N. S. Abbas and S. K. Shukla, *J. Mater. Sci.: Mater. Electron.*, 2020, **31**, 11887–11896.
- 69 G. Poźniak, B. Krajewska and W. Trochimczuk, *Biomaterials*, 1995, **16**, 129–134.
- 70 Ö. Alptekin, *Chem. Pap.*, 2022, **76**, 749–761.
- 71 G. K. Mishra, A. Sharma, K. Deshpande and S. Bhand, *Appl. Biochem. Biotechnol.*, 2014, **174**, 998–1009.
- 72 K. Kim, J. Lee, B. M. Moon, Y. B. Seo, C. H. Park, M. Park and G. Y. Sung, *Sensors*, 2018, **18**, 2607.
- 73 N. Kumar and L. S. B. Upadhyay, *Appl. Biochem. Biotechnol.*, 2020, **191**, 1247–1257.
- 74 K. Ovsejevi, C. Manta and F. Batista-Viera, *Methods Mol. Biol.*, 2013, **1051**, 89–116.
- 75 C. Chatgililoglu, B. Marciniak and K. Bobrowski, *Redox Biochem. Chem.*, 2024, 100046, DOI: [10.1016/j.rbc.2024.100046](https://doi.org/10.1016/j.rbc.2024.100046).
- 76 R. D. Bach, O. Dmitrenko and C. Thorpe, *J. Org. Chem.*, 2008, **73**, 12–21.
- 77 X. Pei, Z. Luo, L. Qiao, Q. Xiao, P. Zhang, A. Wang and R. A. Sheldon, *Chem. Soc. Rev.*, 2022, **51**, 7281–7304.
- 78 S. Jamwal, S. Ranote, U. Dautoo and G. S. Chauhan, *Int. J. Biol. Macromol.*, 2020, **158**, 521–529.
- 79 H. H. Weetall and L. S. Hersh, *Biochim. Biophys. Acta, Enzymol.*, 1969, **185**, 464–465.
- 80 B. Öndeş, F. Akpınar, M. Uygün, M. Muti and D. A. Uygün, *Microchem. J.*, 2021, **160**, 105667.
- 81 H. Choi, S. H. Cho and S. K. Hahn, *ACS Nano*, 2020, **14**, 6683–6692.
- 82 T. Patiño Padial, E. Del Grosso, S. Gentile, L. Baranda Pellejero, R. Mestre, L. J. M. M. Paffen, S. Sánchez and F. Ricci, *J. Am. Chem. Soc.*, 2024, **146**, 12664–12671.
- 83 D. Yang, J. Fan, F. Cao, Z. Deng, J. A. Pojman and L. Ji, *RSC Adv.*, 2019, **9**, 3514–3519.
- 84 M. Şenel, A. Coşkun, M. Fatih Abasıyanık and A. Bozkurt, *Chem. Pap.*, 2010, **64**, 1–7.
- 85 D. Chang, K. Tram, B. Li, Q. Feng, Z. Shen, C. H. Lee, B. J. Salena and Y. Li, *Sci. Rep.*, 2017, **7**, 3110.
- 86 S. M. U. Ali, Z. H. Ibupoto, S. Salman, O. Nur, M. Willander and B. Danielsson, *Sens. Actuators, B*, 2011, **160**, 637–643.

- 87 X. Liang, Q. Li, Z. Shi, S. Bai and Q. Li, *J. Chem. Eng.*, 2020, **28**, 2173–2180.
- 88 J. Song, O. E. Shklyav, A. Sapre, A. C. Balazs and A. Sen, *Angew. Chem., Int. Ed.*, 2024, **63**, e202311556.
- 89 J. Son, S. Parveen, D. MacPherson, Y. Marciano, R. H. Huang and R. V. Ulijn, *Biomater. Sci.*, 2023, **11**, 6457–6479.
- 90 R. H. Huang, N. Nayeem, Y. He, J. Morales, D. Graham, R. Klajn, M. Contel, S. O'Brien and R. V. Ulijn, *Adv. Mater.*, 2022, **34**, 2104962.
- 91 F. Sheehan, D. Sementa, A. Jain, M. Kumar, M. Tayarani-Najjaran, D. Kroiss and R. V. Ulijn, *Chem. Rev.*, 2021, **121**, 13869–13914.
- 92 J. J. Panda and V. S. Chauhan, *Polym. Chem.*, 2014, **5**, 4418–4436.
- 93 T. Li, X. M. Lu, M. R. Zhang, K. Hu and Z. Li, *Bioact. Mater.*, 2022, **11**, 268–282.
- 94 P. Trucillo, R. Campardelli and E. Reverchon, in *Advances in Bionanomaterials: Selected Papers from the 2nd Workshop in Bionanomaterials, BIONAM 2016, October 4-7, 2016, Salerno, Italy*, ed. S. Piotta, F. Rossi, S. Concilio, E. Reverchon and G. Cattaneo, Springer International Publishing, Cham, 2018, pp. 23–35, DOI: [10.1007/978-3-319-62027-5_3](https://doi.org/10.1007/978-3-319-62027-5_3).
- 95 Y. Miele, M. Mella, L. Izzo and F. Rossi, *J. Phys. Chem. Lett.*, 2022, **13**, 1979–1984.
- 96 S. R. Kavanagh, C. N. Savory, S. M. Liga, G. Konstantatos, A. Walsh and D. O. Scanlon, *J. Phys. Chem. Lett.*, 2022, **13**, 10965–10975.
- 97 H. Che, S. Cao and J. C. M. van Hest, *J. Am. Chem. Soc.*, 2018, **140**, 5356–5359.
- 98 W. P. van den Akker, H. Wu, P. L. W. Welzen, H. Friedrich, L. K. E. A. Abdelmohsen, R. A. T. M. van Benthem, I. K. Voets and J. C. M. van Hest, *J. Am. Chem. Soc.*, 2023, **145**, 8600–8608.
- 99 O. Rifaie-Graham, J. Yeow, A. Najer, R. Wang, R. Sun, K. Zhou, T. N. Dell, C. Adrianus, C. Thanapongpibul, M. Chami, S. Mann, J. R. de Alaniz and M. M. Stevens, *Nat. Chem.*, 2023, **15**, 110–118.
- 100 P. Peschke, B. V. V. S. P. Kumar, T. Walther, A. J. Patil and S. Mann, *Chem*, 2024, **10**, 600–614.
- 101 H. Zhou, R. Cheng, M. Quarrell and D. Shchukin, *J. Colloid Interface Sci.*, 2023, **638**, 403–411.
- 102 J. Djonlagić and Z. S. Petrović, *J. Polym. Sci., Part B: Polym. Phys.*, 2004, **42**, 3987–3999.
- 103 T. Godjevargova and K. Gabrovská, *Macromol. Biosci.*, 2005, **5**, 459–466.
- 104 X. Fan and A. Walther, *Angew. Chem., Int. Ed.*, 2021, **60**, 3619–3624.
- 105 G. Fusi, D. Del Giudice, O. Skarsetz, S. Di Stefano and A. Walther, *Adv. Mater.*, 2023, **35**, 2209870.
- 106 J. Erfkamp, M. Guenther and G. Gerlach, *Sensors*, 2019, **19**, 2858.
- 107 I. N. Bujanja, T. Bánsági and A. F. Taylor, *React. Kinet. Mech. Cat.*, 2018, **123**, 177–185.
- 108 P. Zucca, R. Fernandez-Lafuente and E. Sanjust, *Molecules*, 2016, **21**, 1577.
- 109 X. Lyu, R. Gonzalez, A. Horton and T. Li, *Catalysts*, 2021, **11**, 1211.
- 110 I. Maity, C. Sharma, F. Lossada and A. Walther, *Angew. Chem., Int. Ed.*, 2021, **60**, 22537–22546.
- 111 R. W. Jagers and S. A. F. Bon, *J. Mater. Chem. B*, 2017, **5**, 8681–8685.
- 112 F. Muzika, T. Bánsági, I. Schreiber, L. Schreiberová and A. F. Taylor, *Chem. Commun.*, 2014, **50**, 11107–11109.
- 113 R. W. Jagers and S. A. F. Bon, *Mater. Horiz.*, 2017, **4**, 402–407.
- 114 R. W. Jagers and S. A. F. Bon, *J. Mater. Chem. B*, 2017, **5**, 7491–7495.
- 115 V. M. Markovic, T. Bánsági, Jr., D. McKenzie, A. Mai, J. A. Pojman and A. F. Taylor, *Chao*, 2019, **29**, 033130.
- 116 H. El-Samad, *Cell Syst.*, 2021, **12**, 477–487.
- 117 I. Maity, N. Wagner, D. Dev and G. Ashkenasy, *Acc. Chem. Res.*, 2025, **58**, 428–439.
- 118 T. Bánsági, Jr. and A. F. Taylor, *J. Phys. Chem. B*, 2014, **118**, 6092–6097.
- 119 M. M. Wrobel, T. Bánsági, Jr., S. K. Scott, A. F. Taylor, C. O. Bounds, A. Carranza and J. A. Pojman, *Biophys. J.*, 2012, **103**, 610–615.
- 120 E. Jee, T. Bánsági Jr., A. F. Taylor and J. A. Pojman, *Angew. Chem., Int. Ed.*, 2016, **55**, 2127–2131.
- 121 S. Panja, B. Dietrich, O. Shebanova, A. J. Smith and D. J. Adams, *Angew. Chem., Int. Ed.*, 2021, **60**, 9973–9977.
- 122 S. Panja, K. Boháčová, B. Dietrich and D. J. Adams, *Nano-scale*, 2020, **12**, 12840–12848.
- 123 S. Panja and D. J. Adams, *Chem. Commun.*, 2019, **55**, 47–50.
- 124 S. Panja and D. J. Adams, *Chem. Commun.*, 2019, **55**, 10154–10157.
- 125 L. Heinen, T. Heuser, A. Steinschulte and A. Walther, *Nano Lett.*, 2017, **17**, 4989–4995.
- 126 M. S. Long, C. D. Jones, M. R. Helfrich, L. K. Mangeney-Slavin and C. D. Keating, *Proc. Natl. Acad. Sci. U. S. A.*, 2005, **102**, 5920.
- 127 S. Panja and D. J. Adams, *Giant*, 2021, **5**, 100041.
- 128 P. Ravarino, S. Panja, S. Bianco, T. Koev, M. Wallace and D. J. Adams, *Angew. Chem., Int. Ed.*, 2023, **62**, e202215813.
- 129 S. Bianco, F. Hallam Stewart, S. Panja, A. Zyar, E. Bowley, M. Bek, R. Kádár, A. Terry, R. Appio, T. S. Plivelic, M. Maguire, H. Poptani, M. Marcello, R. R. Sonani, E. H. Egelman and D. J. Adams, *Nat. Synth.*, 2024, **3**, 1481–1489.
- 130 A. Llopis-Lorente, M. J. G. Schotman, H. V. Humeniuk, J. C. M. van Hest, P. Y. W. Dankers and L. K. E. A. Abdelmohsen, *Chem. Sci.*, 2024, **15**, 629–638.
- 131 J. Krehan, C.-R. Li, M. Masukawa, E. Amstad and A. Walther, *Chem*, 2025, 102409, DOI: [10.1016/j.chempr.2024.102409](https://doi.org/10.1016/j.chempr.2024.102409).
- 132 B. Dúzs, O. Skarsetz, G. Fusi, C. Lupfer and A. Walther, *Nat. Commun.*, 2024, **15**, 8957.
- 133 M. Tortajada, D. Ramón, D. Beltrán and P. Amorós, *J. Mater. Chem.*, 2005, **15**, 3859–3868.
- 134 A. Norouzian Baghani, A. H. Mahvi, M. Gholami, N. Rastkari and M. Delikhoon, *J. Environ. Health Sci. Eng.*, 2016, **14**, 11.
- 135 N. R. Mohamad, N. H. Marzuki, N. A. Buang, F. Huyop and R. A. Wahab, *Biotechnol. Biotechnol. Equip.*, 2015, **29**, 205–220.
- 136 J. M. Bolivar and B. Nidetzky, *Molecules*, 2019, **24**, 3460.
- 137 N. J. Greenfield, *Nat. Protoc.*, 2006, **1**, 2891–2899.

- 138 T. Prabhakar, J. Giaretta, R. Zulli, R. J. Rath, S. Farajikhah, S. Talebian and F. Dehghani, *Chem. Eng. J.*, 2025, **503**, 158054.
- 139 S. Panja and D. J. Adams, *Chem. – Eur. J.*, 2021, **27**, 8928–8939.
- 140 A. Liese and L. Hilterhaus, *Chem. Soc. Rev.*, 2013, **42**, 6236–6249.
- 141 R. C. Rodrigues, C. Ortiz, Á. Berenguer-Murcia, R. Torres and R. Fernández-Lafuente, *Chem. Soc. Rev.*, 2013, **42**, 6290–6307.